AIAA Journal

VOLUME 2 MAY 1964 NUMBER 5

Structural Analysis of Viscoelastic Materials

M L Williams
California Institute of Technology, Pasadena, Calif

1 Introduction

A FEW years ago, the author drew attention to the growing importance of viscoelastic analysis in evaluating the structural integrity of solid propellant rocket motors [1 2] Although viscoelastic materials have been incorporated as structural elements in many engineering situations, as, for example, in asphalt pavements, their greatest recent application, which has provided the stimulus for accompanying analyses, has certainly been due to the increasing use of viscoelastic solid fuels in rockets As described in the pre ceding papers, this fuel is characteristically of two types: double-base or composite The former is essentially an equal-part mixture of solvent, nitroglycerin, and nitrocellulose cast or extruded into the desired shape, whereas the latter is composed of three-quarters relatively hard, but small, oxidizer particles embedded in the remaining one-quarter rubber fuel matrix In both cases, the elastomeric content is sufficiently large to cause the mixture to possess significant time-dependent properties

At the outset it should be recognized that the medium is not the assumed isotropic-homogeneous continuum on the microscale Nevertheless, for analysis purposes, it will be treated as such in much the same way as concrete aggregate, asphalt, or, for that matter, metals In the gross sense, such an assumption is permissible with important exceptions, such as stress-induced anisotropy and fracture origins, treated separately

The difference between viscoelastic media and more common elastic ones lies essentially in the relation between stress and strain Whereas normal elastic analyses are based upon a (spring) constant proportionality between the two, with Young's modulus as the proportionality constant, the more general viscoelastic relation must allow for time or strain-rate effects Conceptually, it turns out that the easiest way to incorporate rate effects into the mathematical model is to provide dashpot elements in addition to the elastic spring elements In this way, an arbitrary stress-strain time relation can be represented by increasing numbers of spring-dashpot elements having responses over a wide spectrum of spring or rate sensitivities The least amount of analytical complexity is introduced if the material is linearly viscoelastic Such behavior implies that, at any instant, the magnitude of a time-dependent response is directly proportional to the magnitude of the applied time-dependent input Fortunately, this assumption has proved sufficiently precise for most solid propellant materials Thus, one is permitted to assume that the spring and dashpot characteristics depend at most on temperature, and that no nonlinear coupling occurs in the stress-strain law Although the use of discrete spring and dashpot element representation is conceptually convenient, quantitative accuracy over large time ranges usually requires an inordinately large number of such elements that algebraically complicate the analysis As an alternative, therefore, one can develop a method for approximating the broad-band time response, wherein detailed accuracy at any one time is sacrificed in order to obtain reasonable representation over the complete time scale between the short-time (glassy) behavior and long-time (rubbery) behavior This approach leads to what is ordinarily

Professor Williams has taught various courses in flight testing, systems engineering, and solid mechanics at the Firestone Flight Sciences Laboratory at the California Institute of Technology, since receiving his doctorate there in 1950 His research interests have been concentrated primarily in fractu e mechanics which, in the past few years, has extended to studies of fracture in the nonmetals These studies have required a quantitative mechanical and optical characterization of viscoelastic media and have led to the present survey paper He was Vice-Chairman of the Joint Army-Navy-Air Force (JANAF) Physical Prope ties Panel, and the first chairman of its Structural Integrity Committee As an Associate Fellow of the Institute of Aerospace Sciences, he was active in the Student Activities Committee He was also a Senior Member of the American Rocket Society, and a member of the Propellant and Combustion, Structures and Materials, and Solid Rockets Technical Committees He is an Associate Fellow Member of AIAA, and he holds present appointments to the AIAA Committee on Structures and the Committee on Solid Rockets

Presented as Preprint 63-284 at the AIAA Summer Meeting, Los Angeles, Calif , June 17–20, 1963; revision received November 21, 1963 Certain parts of the Graduate Aeronautical Laboratories, California Institute of Technology work reviewed in the paper were supported by a grant from NASA, Office of Grants and Research Contracts, and by the U S Air Force, Aerospace Research Laboratories, Office of Aerospace Research

called a spectral distribution of characteristic relaxation or retardation times; and, among other uses, it is convenient for preliminary design-type analysis where there may be only limited mechanical property data as, for example, in the case of new propellant formulations

Having noted that the main new effect in viscoelastic analysis is incorporated in the stress-strain law, and having mentioned that one normally characterizes its behavior in terms of a finite-element model or a spectral representation, it is appropriate next to make some general statements as to how viscoelastic stress analysis is conducted As summarized in the earlier papers,[1,2] the essential feature is the existence of a "correspondence rule," originally proposed by Alfrey[3] for an incompressible material wherein, for most problems of engineering interest, Laplace transformations can be taken of the time-dependent variables and forcing functions to obtain an associated elasticity problem in the transformed variables The solution of this problem, when transformed back into the real time variables, gives the desired result In practice, this technique is first complicated by the basic necessity of having to solve the (associated) elasticity boundary-value problem, i e , the elasticity solution to a given problem is usually an a priori requirement to a viscoelasticity solution, and if the elasticity solution is untractable, as in some three-dimensional geometries, the viscoelasticity solution will be more so In addition to this fundamental but usual difficulty, two others arise The first is the manner in which the viscoelastic stress-strain law is to be introduced into the associated problem, with the complexity approximately proportional to the number of discrete spring-dashpot elements used in the material representation The second is the mathematical problem of inverting the associated problem to obtain the physical solution As is well known, the basic inversion process usually involves contour integration or residue theory with its complexity depending upon the poles of the function being inverted It develops, however, that the character of viscoelastic deformations is such that most of the poles lie upon the negative real axis Schapery[4] has taken advantage of this fact to develop an important approximate inversion technique that permits a relatively straightforward calculation, irrespective of the complexity of material representation

Considerable recent progress in viscoelastic analysis has been made, but it is appropriate nevertheless to point out that the problem of transient thermal viscoelastic stress analysis, as in thermal cycling or grain curing, is significantly more complicated than that for isothermal conditions Practically speaking, this problem is still basically untractable, although several authors, following the initial Morland and Lee[5] formulation, have concerned themselves with engineering applications The heart of the problem lies in the sensitivity of the stress-strain law to temperature changes, particularly in the dashpot elements The nature of difficulty is qualitatively similar to the difference between solving a linear differential equation with constant vs variable coefficients In the physical situation, the material properties are changing simultaneously with the transient temperature distribution through the body This problem area is expected to require additional effort before a completely satis factory engineering analysis will have been attained

Accepting for the moment that one could carry out a stress analysis for a given loading, specified material, and geometrical configuration, it is still necessary to combine the stress distribution with a failure criterion in order to evaluate the structural integrity of a design As in the last surveys, it is still impossible to state categorically a unique failure criterion in terms of stress, strain, or combinations thereof To restate the position, the majority of experimentally determined failure data has been obtained under conditions of uniaxial tension, although over a complete range of strain rate and temperature [Actually a "reduced strain-rate" parameter $Ra_T(T)$ has been used because it is characteristic that the dependence is basically upon the product of actual constant strain rate R and an experimentally determined temperature shift factor a_T] On the other hand, it is evident that in most geometries of engineering interest the stress or strain distribution is multiaxial Although, in metals, experience has shown how to correlate uniaxial and multiaxial states as for example, using the octahedral stress (von Mises) criterion, such connection has not yet been sufficiently well established for viscoelastic materials Fur thermore, another complication arises because of the strain-rate dependence

If, for argument's sake, one considers the three-dimensional failure space in terms of the three principal stress axes, one could plot the uniaxial failure stress at a given constant strain rate R along one of the coordinate axes Further, assuming isotropic failure, this same point also could be plotted on the other two axes $\sigma_1 = \sigma_u$ and $\sigma_2 = \sigma_3 = 0$ with the indices permuting Then, if one had failure data for other multiaxial stress states at comparable strain rates (hydrostatic tension, for example, wherein $\sigma_1 = \sigma_2 = \sigma_3 = \sigma_T$, corresponding to a point on the vector, bisecting the 1, 2, 3 axes), it would be possible to construct a failure surface for the given strain rate If it turned out, for instance, that $\sigma_T = \sigma_u/3^{1/2}$, the first octant failure surface could be a sphere with radius $\sigma_u(R)$ Note, however, that, because R is a parameter, there would be, in general, a new distinct surface for each different strain rate (in this case more or less like layers of onion skins) Hence, instead of a simple correlation between uniaxial and multiaxial states as in the von Mises correlation for metals, the association of multiaxial states for viscoelastic materials must also include strain rate

The other important shortcoming of failure analysis relates to behavior under varying strain rate As previously mentioned, most testing has been conducted at *constant* strain rate to failure On the other hand, actual loading conditions will normally impose a *varying* strain rate on the body in question It is a fair question to inquire how one might predict failure in the latter situation given only the former data Although Williams[2] has proposed a cumulative damage law analogous to the Miner law for fatigue, it suffers inherently from many of the same type of deficiencies and has led Knauss[6] to a consideration of the micromechanisms involved and the possibility of a significantly improved treatment

In concluding these introductory remarks, it is pertinent to comment upon two other items specifically pertinent to the viscoelastic analysis of solid propellant rocket motors The first of these relates to the stress analysis of thick-walled cylinders with special reference to three-dimensional end effect and finite length Recall first the statement that an elastic solution is usually the prerequisite to a viscoelastic one In this connection Parr and Gillis[7] and Messner[8] have programmed numerical solutions by which one is now able to evaluate the deviation from simple (infinite length) plane strain results In particular, one can now, at least for flat-ended cylinders,[7] read from design charts the central stresses and strains, choking deflections and bond-end loads for a variety of loading conditions, web fractions, material properties, and length-to-diameter ratios Further, using the Schapery inversion, this digital data now can be extended, in conjunction with property data, to the viscoelastic situation

The other item represents an interesting design consideration, formerly restricted to the automobile tire industry, brought to the attention of the rocket industry by Tormey and Britton[9] In some rather startling photographs, they have demonstrated that, if viscoelastic materials are vibrated as during flight, transportation, or handling conditions, they may generate sufficient heat as a result of cumulative viscous dissipation to degrade the material significantly, even to the point that the material flows Although the basic phenomenon is not new and can be related directly to an interaction

between the natural frequency of the configuration and the imaginary part of the complex shear modulus (loss tangent), its possible occurrence in rocket motors should be noted by designers and suitable analytical and experimental action taken

In proceeding now into a more detailed consideration of some of the points discussed, certain aspects of the presentation and organization of material will follow the comprehensive report prepared by the author and his colleagues, Blatz and Schapery,[10] relating to the structural integrity evaluation of solid rocket grains, which important collaboration is gratefully acknowledged

2 Material Characterization

In an isotropic homogeneous elastic body, there are only two independent material constants that, without loss of generality, can be taken as the bulk modulus K, relating the dilatation stress and dilatation strain, and the shear modulus G, relating the shear stress and strain Specifically, let the deviatoric stress and strain components be s_{ij} and e_{ij}, respec tively, such that

$$s_{ij} = \sigma_{ij} - (\tfrac{1}{3})\delta_{ij}\sigma_{kk} \tag{2 1}$$

$$e_{ij} = \epsilon_{ij} - (\tfrac{1}{3})\delta_{ij}\epsilon_{kk} \tag{2 2}$$

where σ_{ij} and ϵ_{ij} are the usual stress and strain components The deviatoric stresses, therefore, are those from which the hydrostatic component has been subtracted In this form, the distortion, or shear relation, becomes

$$s_{ij} = 2Ge_{ij} \tag{2 3}$$

and the dilatation, or bulk relation becomes

$$\sigma_{ii} = 3K\,\epsilon_{ii} \tag{2 4}$$

Turning now to the conditions in a linearly viscoelastic medium, it is convenient to interpret the isothermal stress-strain relation in the linear differential operator form which can be associated with a combination of springs and dashpots, namely,

$$[a\,\partial^n/\partial t^n + \quad + a_0]s_{ij}(x_k,t) = [b_m\partial^m/\partial t^m + \quad + b_0]e_{ij}(x_k,t) \tag{2 5}$$

$$[c_i\partial/\partial t + \quad + c_0]\sigma_{ii}(x_k,t) = [d\,\partial/\partial t + \quad + d_0]\epsilon_{ii}(x_k,t) \tag{2 6}$$

wherein the material constants a_n, b_m, c, and d are to be determined from experimental measurements as, for example, fitting the stress response to specified bulk and shear inputs Bypassing for the moment a more detailed description of their determination, consider the Laplace transforms of (2 5) and (2 6) for zero initial conditions,

$$\bar{s}_{ij}(x_k,p) = \frac{[b_m p^m + \quad + b_0]}{[a\,p^n + \quad + a_0]}\,\bar{e}_{ij}(x_k,p) \equiv 2G(p)\bar{e}_{ij}(x_k,p) \tag{2 7}$$

$$\bar{\sigma}_{ii}(x_k,p) = \frac{[d_s p + \quad + d_0]}{[c\,p + \quad + c_0]}\,\bar{\epsilon}_{ii}(x_k,p) \equiv 3K(p)\bar{\epsilon}_{ii}(x_k,p) \tag{2 8}$$

or their inverses,

$$2\bar{e}_{ij}(x_k,p) \equiv J(p)\bar{s}_{ij}(x_k,p) \tag{2 9}$$

$$3\bar{\epsilon}_{ii}(x_k,p) \equiv B(p)\bar{\sigma}_{ii}(x_k,p) \tag{2 10}$$

which reveal the pseudoelastic character of the stress-strain law in the transform plane by comparison with (2 3) and (2 4) The purpose of material characterization is to determine the nature of $G(p)$ and $K(p)$ in a convenient form that can then be used in subsequent stress analysis It may be noted in passing that, if these two characterizations are given, the other commonly used (associated) material quantities can be found from

$$E(p) = \frac{9G(p)K(p)}{3K(p) + G(p)} \tag{2 11}$$

$$\nu(p) = \frac{3K(p) - 2G(p)}{6K(p) + 2G(p)} \tag{2 12}$$

The Incompressibility Assumption

It is customary to assume that rubbery materials are essentially incompressible, which for small strains is equivalent to assuming an infinite bulk modulus or a Poisson's ratio of one-half Because the precise measurement of compressibility is not yet commonplace in most laboratories, it is pertinent to dwell for a moment upon three basic stages of approximation to the material behavior The first is the one already mentioned—incompressibility in bulk but permitting viscoelastic shear behavior The second permits a finite value of the bulk modulus but neglects any time dependence, thus replacing its actual time-dependent behavior by an average constant (elastic) value The shear behavior is assumed viscoelastic as before The last stage is to assume that both bulk and shear are viscoelastic, with the approximation lying solely in linearity, isotropy, and homogeneity

The first case gives, therefore,

$$K(p) = \infty \qquad \nu(p) = \tfrac{1}{2} \qquad E(p) = 3G(p) \tag{2 13}$$

whereas the second gives

$$K(p) = K \qquad \nu(p) = \frac{3K_e - 2G(p)}{6K + 2G(p)} \qquad E(p) = \frac{9K\,G(p)}{3K + G(p)} \tag{2 14}$$

and the incorporation of either assumption usually depends upon the availability of experimental data

Characterization Methods

In an elastic body, the material parameters, for example, the Young's modulus E, can be determined through one of several tests as convenient to the experimenter Although it is customary to test uniaxial bars in tension, it is equally possible to measure E by bending a narrow cantilever beam Similarly, for viscoelastic media one determines $G(p)$ and $K(p)$ by some test convenient to the experimentalist For these purposes four are commonly used: 1) step-strain input, measure stress-relaxation output; 2) step-stress input, measure creep-strain output; 3) constant strain-rate input, measure stress output; and 4) sinusoidal-stress (strain) input, measure strain (stress) output Any of these may be selected, although practical limitations usually cause the data to be more reliable in some time regions than others, thus requiring two or more tests, perhaps overlapping in their time ranges of applicability, to characterize completely the response for all times between zero and infinity

As a case in point, test 1 of the forementioned calls for a mathematically sharp step-strain input One attempts to achieve this condition in the laboratory in a "trap-door" reaction by displacing the end of a tensile specimen a finite distance in zero time Hence, as a practical matter, there is always a minimum rise time of the order of milliseconds below which the strain has not reached full value If faster displacements are imposed, say by explosive caps, inertia effects normally disregarded may be introduced Such limitations, therefore, lead to poor resolutions at very short times On the other hand, a sinusoidal high-frequency oscillation is quite practical and permits one to fill out the

short-time end of the time scale by combining two tests instead of relying solely upon one

It is important to note, however, that the four common tests just enumerated are not exhaustive by any means It suffices to impose a completely known input and measure completely the response in order to determine the operator $G(p)$ or $K(p)$ For example, if one were to impose a known ramp strain input from zero time to 1 msec, and constant thereafter, and simultaneously measure the stress relaxation carefully from zero time, then, in principle, the transforms of the input and output data could be computed, numerically if need be, and the division of one by the other would completely specify the material property operator Indeed, appreciating the indeterminacy of the applied strain at short times, Francis and Cantey[11] have used the actual partial ramp input in obtaining the shear operator It is worth emphasizing that the selection of a particular test, one of the forementioned or another, becomes solely a matter of experimental accuracy, not one of principle

It has already been indicated that alternative assumptions regarding compressibility can be introduced For the purpose of illustration in terms of the principal stresses and strains take

$$\left[\frac{\bar{\sigma}_1(p) - \bar{\sigma}_2(p)}{2}\right] = G(p)[\bar{\epsilon}_1(p) - \bar{\epsilon}_2(p)] \qquad (2\ 15)$$

and consider a simple uniaxial tension test of an incompressible material Thus, $\sigma_1 = \sigma$, $\sigma_2 = 0$, $\epsilon_1 = \epsilon$, $\epsilon_2 = -\nu\epsilon_1$ for $\nu = \frac{1}{2}$, or

$$\bar{\sigma}(p) = 3G(p)\bar{\epsilon}(p) = E(p)\bar{\epsilon}(p) \qquad (2\ 16)$$

This relation will be used in several examples and is, of course, the viscoelastic analog of the uniaxial elastic tension test

Stress relaxation

Assuming perfection in the experiment such that $\epsilon(t) = \epsilon_0$ for $t > 0$, then $\bar{\epsilon}(p) = \epsilon_0/p$ Upon defining the relaxation modulus

$$E_{el}(t) \equiv \sigma_{el}(t)/\epsilon_0 \qquad \bar{E}_{el}(p) = \bar{\sigma}_{el}(p)/\epsilon_0 \qquad (2\ 17)$$

as the normalized stress relaxation to the step strain, one has, using (2 16),

$$\bar{\sigma}_{\ 1}(p) = E(p)[\epsilon_0/p]$$

giving

$$E(p) = p\bar{E}_{el}(p) \qquad (2\ 18)$$

Creep

In a similar fashion, but beginning with (2 9) and noting that the inverse of $E(p)$ is defined as the compliance $D(p)$, one finds that, due to a step-stress input $\sigma(t) = \sigma_0$, then $\bar{\sigma}(p) = \sigma_0/p$ Upon defining the creep compliance

$$D_{\ p}(t) \equiv \epsilon_{c\ p}(t)/\sigma_0 \qquad \bar{D}_{c\ p}(p) = \bar{\epsilon}_{crp}(p)/\sigma_0 \qquad (2\ 19)$$

as the normalized creep response to an applied step stress, one has, upon inverting (2 16),

$$\bar{\epsilon}(p) = D(p)\bar{\sigma}(p) \qquad (2\ 20)$$

leading to

$$D(p) = p\bar{D}_{c\ p}(p) \qquad (2\ 21)$$

Constant strain rate

This test is commonly used because it is mechanistically possible to design a fairly satisfactory testing machine to impose a constant cross head speed, which, within a reasonable approximation, gives a constant strain rate R in a tensile specimen Thus, one requires $\epsilon(t) = Rt$ or $\bar{\epsilon}(p) = R/p^2$, and the stress response is $\sigma_{t\ n}(t)$, such that (2 16) gives

$$[p\bar{\sigma}_{t\ n}(p)/R] = [E(p)/p] = \bar{E}_{\ 1}(p) \qquad (2\ 22)$$

using (2 18) The left term, however, is the transform of the slope of the tensile stress strain curve during the constant strain-rate test,

$$\mathfrak{L}[d\sigma_{t\ n}(t)/Rdt] = p\bar{\sigma}_{t\ n}(p)/R \qquad (2\ 23)$$

which is precisely the relaxation modulus,

$$[d\sigma_{t\ n}(t)/d\epsilon]_{\epsilon = Rt} = E_{\ 1}(t) \qquad (2\ 24)$$

Dynamic response

This experimental technique consists in applying an oscillating stress or strain input at constant frequency Returning to the linear differential operator form of (2 16) as in (2 5), one has

$$[a_n\partial^n/\partial t^n + \quad + a_0]\sigma(t) = 3[b_m\partial^m/\partial t^m + \quad + b_0]\epsilon(t) \qquad (2\ 25)$$

There are two possibilities: 1) the strain is specified as $\epsilon_0 e^{i\omega t}$, where ϵ_0 is real representing the maximum amplitude of the sine wave, and the response is $\sigma^* e^{i\omega t}$ with σ^* a complex function of frequency, or 2) the opposite situation with the stress prescribed as $\sigma_0 e^{i\omega t}$ and strain as $\epsilon^* e^{i\omega t}$

Upon substituting into (2 25) for the first alternative, one finds

$$[a_n(i\omega) + \quad + a_0]\sigma^* e^{i\omega t} = 3[b_m(i\omega)^m + \quad + b_0]\epsilon_0 e^{i\omega t}$$

so that, upon incorporating the definition of complex modulus, one has

$$\frac{\sigma^*(\omega)}{\epsilon_0} \equiv E^*(\omega) \equiv E'(\omega) + iE''(\omega) = \frac{3[b_m(i\omega)^m + \quad + b_0]}{[a_n(i\omega)^n + \quad + a_0]} \qquad (2\ 26)$$

Similarly, the complex compliance to the stress input is conveniently defined as

$$\epsilon^*(\omega)/\sigma_0 \equiv D^*(\omega) \equiv D'(\omega) - iD''(\omega) = [1/E^*(\omega)] \qquad (2\ 27)$$

It is also convenient to write the complex modulus and compliance in terms of magnitude and phase angle

$$E^*(\omega) = |E^*|e^{i\delta} = [(E')^2 + (E'')^2]^{1/2}e^{i\delta} \qquad (2\ 28)$$

$$D^*(\omega) = |D^*|e^{-i\delta} = [(D')^2 + (D'')^2]^{1/2}e^{-i\delta} \qquad (2\ 29)$$

where the reciprocity (2 27) requires that

$$|E^*|\ |D^*| = 1 \qquad (2\ 30)$$

and the lag angle δ is given by

$$\delta = \tan^{-1}[E''(\omega)/E'(\omega)] = \tan^{-1}[D''(\omega)/D'(\omega)] \qquad (2\ 31)$$

Mathematical Representations

Having described four tests by which $G(p)$, and by an obvious extension $K(p)$, may be determined, let us consider specific alternate mathematical representations of these quantities The first of these is by discrete mechanical elements, the second by continuous spectral representation, and the third by broad band characterization

Discrete element models

The simplest elements are, of course, the Hookean spring and the Newtonian dashpot Their behavior, as well as that of their parallel (Voigt) and series (Maxwell) arrange-

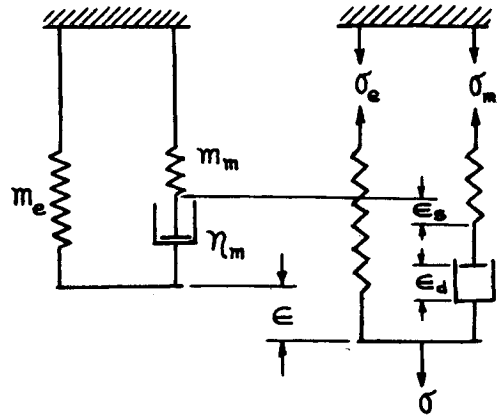

$$\epsilon = \epsilon + \epsilon_d \quad \text{(a)}$$

$$\sigma = \sigma + \sigma_m \quad \text{(b)}$$

where

$$\frac{d\epsilon_s}{dt} = \frac{1}{m_m}\frac{d\sigma_m}{dt} \quad \text{(c)}$$

$$\frac{d\epsilon_d}{dt} = \frac{\sigma_m}{\eta_m} \quad \text{(d)}$$

$$\epsilon = \frac{\sigma_e}{m} \quad \text{(e)}$$

Operator equation

$$\sigma(t) = \left[m + \frac{m_m \frac{d}{dt}}{\left(\frac{d}{dt} + \frac{1}{\tau_m}\right)} \right] \epsilon(t)$$

or

$$\sigma(t) = \frac{m_g\left(\frac{d}{dt} + \frac{m_e}{m_g}\frac{1}{\tau_m}\right)}{\left(\frac{d}{dt} + \frac{1}{\tau_m}\right)} \epsilon(t)$$

where

$$\tau_m = \frac{\eta_m}{m_m}$$

$$m_m + m_e = m_g$$

Creep and recovery

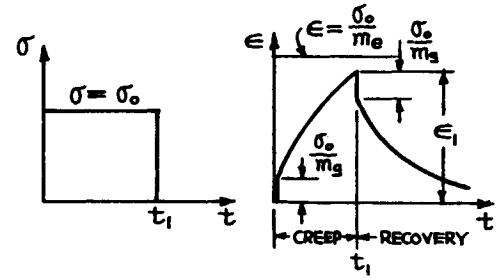

$$\epsilon = \left[1 - \left(1 - \frac{m_e}{m_g}\right)\exp\left(-\frac{m_e}{m_g}\frac{t}{\tau_m}\right)\right]\frac{\sigma_0}{m_e} \text{ for } 0 < t \leq t_1$$

$$\epsilon = \left[\epsilon_1 - \frac{\sigma_0}{m_g}\right]\exp\left(-\frac{m_e}{m_g}\frac{(t - t_1)}{\tau_m}\right) \text{ for } t > t_1$$

Relaxation

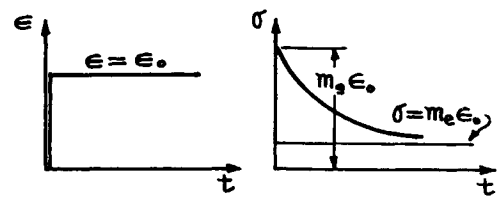

$$\sigma = \left[1 + \left(\frac{m_g}{m_e} - 1\right)e^{-t/\tau_m}\right] m\,\epsilon_0 \text{ for } t > 0$$

Constant strain rate

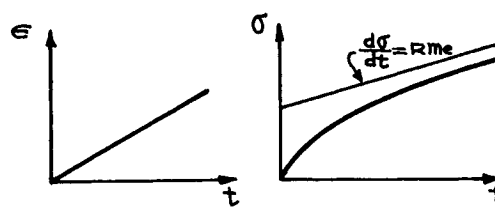

$$\epsilon = Rt$$

(R = strain rate)

$$\sigma = \left[\frac{t}{\tau_m} + \left(\frac{m_g}{m} - 1\right)(1 - e^{-t/\tau_m})\right] Rm\,\tau_m$$

Fig 1 Three-element model: Maxwell and Spring

ments, was summarized earlier [1] From the physical standpoint it is important to recognize that the Maxwell arrangement of the two elements in series corresponds to an unlimited deformation under load similar to that occurring in an uncross-linked polymer On the other hand, the Voigt arrangement, providing for a maximum displacement limited by the elastic deformation of the spring, corresponds physically to a cross-linked polymer In the latter case, the individual long polymer chains possess cross ties, which permit significantly greater shear rigidity In a qualitative way, uncross-linked polymers as polyisobutylene have unlimited deformation, whereas cross-linked systems as polyurethane are stiffer and possess a finite long-time rubbery modulus (Photoelasticians may recognize that the soft sensitive birefringent material Hysol is a member of the urethane family)

The simplest model to possess most of the general features of viscoelastic deformation is the typical three-element model shown in Fig 1 It exhibits an instantaneous glassy response as well as delayed elasticity and recovery As has been intimated earlier, there are unfortunately only three material constants, two spring constants and one dashpot viscosity, with which to curve fit the response of an actual material, and it would be highly unlikely that they would be sufficient in the general case Nevertheless, for a very restricted range of time, or for qualitative demonstration of viscoelastic effects, it is very useful The first thought in improving finite element accuracy is to increase the number of elements This subject has been investigated by many authors, and Elder[12] has recently completed a comprehensive study that included as many as 8–10 elements Although

$$\epsilon = \epsilon_{si} + \epsilon_{di} \quad \text{(a)}$$

$$\sigma = \sigma + \sum_{i=1}^{n} \sigma_i \quad \text{(b)}$$

where

$$\frac{d\epsilon}{dt} = \left[\frac{1}{m_i}\frac{d}{dt} + \frac{1}{\eta_i}\right]\sigma_i \quad \text{(c)}$$

$$\epsilon = \frac{\sigma_e}{m} \quad \text{(d)}$$

Operator equation

Using (c) and (d) in (b),

$$\sigma(t) = \left[m + \sum_{i=1}^{n} \frac{m_i}{\left(\frac{d}{dt} + \frac{1}{\tau_i}\right)}\left(\frac{d}{dt}\right)\right]\epsilon(t) \quad \text{(e)}$$

where $\tau_i = \dfrac{\eta_i}{m_i}$ $\qquad m_g - m = \sum_{i=1}^{n} m_i$ (f)

To obtain integral representation, let

$$m_i = H(\tau_i)(\Delta_i\tau/\tau_i) \quad \text{(g)}$$

and take the limit

$$\lim_{\substack{n\to\infty \\ \Delta_i\tau\to 0 \\ 0<\tau<\infty}} \sum_{i=1}^{n} \frac{H(\tau_i)\Delta_i\tau}{\left(\frac{d}{dt} + \frac{1}{\tau_i}\right)\tau_i} = \int_0^\infty \frac{H(\tau)}{\left(\frac{d}{dt} + \frac{1}{\tau}\right)\tau} d\tau \quad \text{(h)}$$

Operator equation for an infinite number of elements:

$$\sigma(t) = \left[m + \int_0^\infty \frac{H(\tau)}{\left(\frac{d}{dt} + \frac{1}{\tau}\right)\tau} d\tau \left(\frac{d}{dt}\right)\right]\epsilon(t) \quad \text{(i)}$$

where $H(\tau) \equiv$ relaxation spectrum

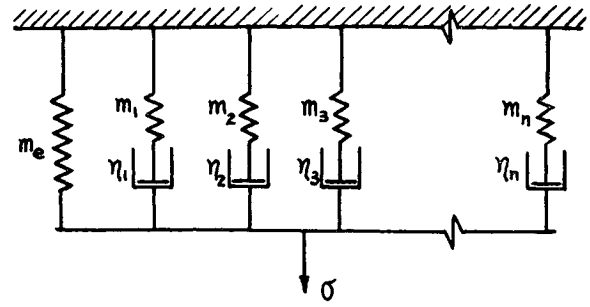

Relaxation

$\epsilon = \epsilon_0$ for $t > 0$

$$\sigma(t) = \left[m + \int_0^\infty \frac{H(\tau)e^{-t/\tau}}{\tau} d\tau\right]\epsilon_0$$

$\left[m + \int_0^\infty \frac{H(\tau)e^{-t/\tau}}{\tau} d\tau\right] \equiv m(t) \equiv$ relaxation modulus

where $m_g - m = \int_0^\infty \frac{H(\tau)}{\tau} d\tau$

because stress responds to the glassy modulus at zero time, i e ,

$$\sigma(0) = \left[m + \int_0^\infty \frac{H(\tau)}{\tau} d\tau\right]\epsilon_0 = m_g\epsilon_0$$

Constant strain rate

$\epsilon = Rt$ $\qquad \sigma(t) = \left[m\,t + \int_0^\infty H(\tau)(1 - e^{-t/\tau})d\tau\right]R$

Differentiating this equation with respect to time yields

$$d\sigma/dt = Rm(t) \quad \text{or} \quad d\sigma/d\epsilon = m(\epsilon/R)$$

where σ = stress in constant strain rate test

Fig 2 Wiechert model

the accuracy over larger time intervals did indeed increase, one must remember that one of the important purposes of the data representation is to use the final mathematical formula for, say, $E(p)$ [Eq (2 7)], in stress analysis As $G(p)$ is the ratio of polynomials which require subsequent Laplace inversion, the computations can become rather unwieldly

Spectral representation

If one passes to the extreme of an infinite number of elements, it develops that, in some ways, a simpler result in terms of a relaxation spectrum can be obtained Figure 2 shows the result for an infinite array of Maxwell elements in parallel plus an equilibrium spring (Wiechert model) An extension of the force and deformation balance as used in the three-element equation to the n element situation gives, in operator form,

$$\sigma(t) = \left\{E_e + \Sigma \frac{m_i}{(d/dt) + (1/\tau_i)} \frac{d}{dt}\right\}\epsilon(t) \quad (2\,32)$$

where the relaxation time of the ith spring is $\tau_i = \eta_i/m_i$ Corresponding to each relaxation time t_i, there is a definite spring constant m_i and viscosity η_i Thus, one can associate or postulate a function $m_i = m_i(\eta_j) = m_i(\tau_j)$ that becomes continuous as the number of elements or increments at $\Delta\tau$ increase without bound A convenient form is found to be

$$m_i = [H(\tau_i)/\tau_i]\Delta_i\tau \quad (2\,33)$$

so that, upon substitution into (2 32) and passage to the limit, there results

$$\sigma(t) = \left\{E + \int_0^\infty \frac{H(\tau)d\tau}{[(d/dt) + (1/\tau)]\tau} \frac{d}{dt}\right\}\epsilon(t) \quad (2\,34)$$

in which $H(\tau)$ is known as the relaxation spectrum, and E is the long-time elastic or rubbery modulus It is thus seen that, instead of having to determine an infinite number of experimental constants m_i and η_i, the problem has been traded for one of determining a suitable function $H(\tau)$ In any event the basic problem remains the same A known input $\epsilon(t)$ is imposed and the resulting response $\sigma(t)$ measured: with $\sigma(t)$ and $\epsilon(t)$ known, $H(\tau)$ is then found as the result of solving the integral equation

Broad-band approximations

As a practical matter, however, it is more expedient to guess various functional forms for $H(\tau)$, integrate, and compare with the experimental data If they do not agree well, try a new assumed form for $H(\tau)$ In this way, and guided by an understanding of polymer mechanics, one can assume $H(\tau)$ to be of the form

$$H(\tau) = c(\tau_0/\tau)^n \exp(-\tau_0/\tau) \quad (2\,35)$$

which is commonly known as the modified power law variation Suppose, for illustrative purposes, that one of the forementioned four tests is run on a given material, e g , constant strain, $\epsilon(t) = \epsilon_0$ In this case, after Laplace transformation, (2 34) becomes

$$\bar{\sigma}(p) = \left\{E_e + \int_0^\infty \frac{H(\tau)d\tau}{p\tau + 1} p\right\}\frac{\epsilon_0}{p} \quad (2\,36)$$

$$\epsilon = \epsilon_g + \sum_{i=1}^{n} \epsilon_i \quad \text{(a)}$$

$$\sigma = \sigma_i + \sigma_{di} \quad \text{(b)}$$

where

$$\frac{d\epsilon_i}{dt} = \phi_i \sigma_{di} \quad \text{(c)}$$

$$\epsilon_i = k_i \sigma_{si} \quad \text{(d)}$$

$$\sigma = \left[\frac{1}{\phi_i}\frac{d}{dt} + \frac{1}{k_i}\right]\epsilon_i \quad \text{(e)}$$

$$\epsilon_g = k_g \sigma \quad \text{(f)}$$

Operator equation

$$\epsilon(t) = \left[k_g + \sum_{i=1}^{n} \frac{k_i}{\tau_i\left(\frac{d}{dt} + \frac{1}{\tau_i}\right)}\right]\sigma(t) \quad \text{(g)}$$

where

$$\tau_i = \frac{k_i}{\phi_i} \qquad k - k_g = \sum_{i=1}^{n} k_i \quad \text{(h)}$$

To obtain integral representation let

$$k_i = L(\tau_i)\frac{\Delta_i \tau}{\tau_i} \quad \text{(i)}$$

and take the limit

$$\lim_{\substack{n\to\infty \\ \Delta_i\tau\to 0 \\ 0<\tau<\infty}} \sum_{i=1}^{n} \frac{L(\tau_i)\Delta_i\tau}{\tau_i\left(\frac{d}{dt} + \frac{1}{\tau_i}\right)\tau_i} = \int_0^\infty \frac{L(\tau)}{\left(\frac{d}{dt} + \frac{1}{\tau}\right)\tau^2} d\tau \quad \text{(j)}$$

Operator equation for an infinite number of elements:

$$\epsilon(t) = \left[k_g + \int_0^\infty \frac{L(\tau)}{\left(\frac{d}{dt} + \frac{1}{\tau}\right)\tau^2} d\tau\right]\sigma(t) \quad \text{(k)}$$

$L(\tau) \equiv$ retardation spectrum

Creep

$$\sigma = \sigma_0 \text{ for } t > 0$$

$$\epsilon(t) = \left[k_g + \int_0^\infty \frac{L(\tau)(1 - e^{-t/\tau})}{\tau} d\tau\right]\sigma_0$$

$$\left[k_g + \int_0^\infty \frac{L(\tau)(1 - e^{-t/\tau})}{\tau} d\tau\right] \equiv k(t) \equiv \text{creep compliance}$$

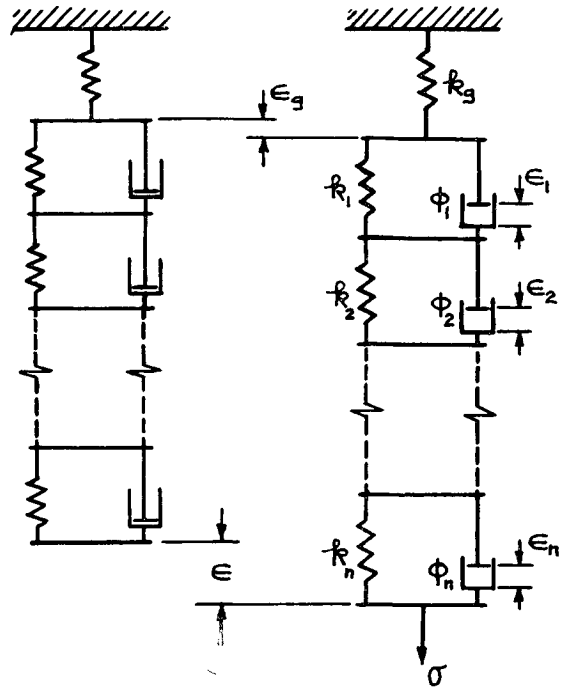

where

$$k - k_g = \int_0^\infty \frac{L(\tau)}{\tau} d\tau$$

Constant stress rate

$$\sigma = Rt$$

$$\epsilon(t) = \left\{kt + \int_0^\infty L(\tau)\left[\frac{t}{\tau} - (1 - e^{-t/\tau})\right]d\tau\right\} R$$

Differentiating this equation with respect to time yields

$$\frac{d\epsilon}{dt} = Rk(t) \qquad \text{or} \qquad \frac{d\epsilon}{d\sigma} = k\left(\frac{\sigma}{R}\right)$$

where ϵ = strain in constant stress rate test

Fig 3 Kelvin model

or, in terms of the relaxation modulus,

$$E_1(t) = E + \int_0^\infty \tau^{-1} H(\tau) \exp\left(\frac{-t}{\tau}\right) d\tau \quad (2\,37)$$

Note that, at short time $t \to 0$, one must obtain physically the glassy or short-time modulus E_g,

$$E_1(0) = E_e + \int_0^\infty \tau^{-1} H(\tau) d\tau = E_g \quad (2\,38)$$

which amounts to a normalizing condition upon the area under the relaxation spectrum curve

Upon substituting the assumed modified power law (2 35) into (2 37), one finds

$$E_1(t) = E + \int_0^\infty \tau^{-1} c \left(\frac{\tau_0}{\tau}\right)^{+n} \exp\left(\frac{-\tau_0}{\tau}\right) \exp\left(\frac{-t}{\tau}\right) d\tau$$

$$= E + \frac{E_g - E_e}{[1 + (t/\tau_0)]^n} \quad (2\,39)$$

where the normalizing condition (2 38) was used to find that [cf Eq (2 35)]

$$c = [(E_g - E)/\Gamma(n)] \quad (2\,40)$$

The relaxation spectrum is therefore given by

$$H(\tau) = \frac{E_g - E_e}{\Gamma(n)}\left(\frac{\tau_0}{\tau}\right)^n \exp\left(\frac{-\tau_0}{\tau}\right) \quad (2\,41)$$

The expression (2 39) for the relaxation modulus is observed to limit-check the glassy and rubbery behavior at short and long times, respectively This broad-band representation is, therefore, seen to possess four arbitrary constants in cluding the limiting moduli values The exponent n gives the slope of the relaxation curve through the transition region between glassy and rubbery behavior, and τ, for isothermal conditions, fixes a characteristic relaxation time

This approximation has been found to be reasonably accurate in several cases, but, before expanding upon this type of broad-band curve fit, it should be mentioned that a similar formula can be developed for a retardation spectrum $L(\tau)$ [which is the inverse form for (2 34)], which is useful when the stress is imposed and the strain is desired [Note that, if the stress was given in (2 34) along with $H(\tau)$, the calculation of the strain was not direct] In this case the infinite array of Voigt elements in series, called a Kelvin model (Fig 3), leads to the general relation

$$\epsilon(t) = \left\{D_g + \int_0^\infty \frac{L(\tau)d\tau}{[(d/dt) + (1/\tau)]\tau^2}\right\}\sigma(t) \quad (2\,42)$$

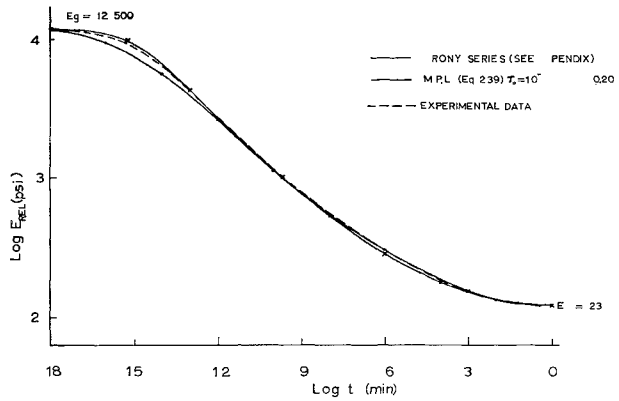

Fig 4a Various representations of relaxation modulus for HC binder

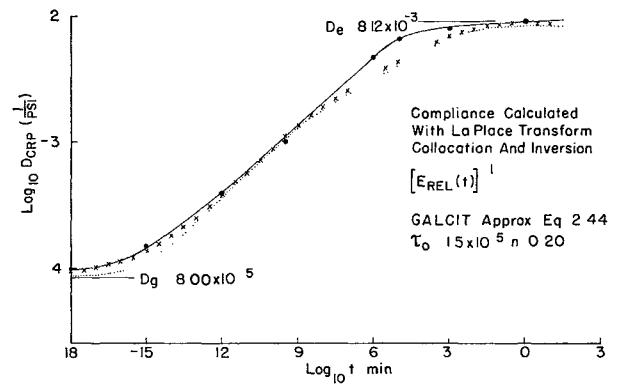

Fig 4b Various representations of creep compliance for HC binder

Recognizing that relaxation and retardation are basically reciprocal, one could also postulate a modified power law for $L(\tau)$ as

$$L(\tau) = c'(\tau/\tau_0)^{n'} \exp(-\tau/\tau_0) \tag{2 43}$$

but the integration for the creep compliance does not give a simple form, and it is more direct to assume a reasonable expression as[10]

$$D_{c\,p}(t) = D_g + \frac{D_e - D_g}{[1 + (\tau_0'/t)]^n} \tag{2 44}$$

where n may be the same exponent as in the relaxation modulus and τ_0' is chosen for the best fit of the data or matching the reciprocal value of the relaxation modulus at the center of the transition region Note that the limiting compliances at short and long times, $D_g = 1/E_g$ and $D = 1/E_e$, respectively, are satisfactorily obtained in (2 44)

Interrelation of creep compliance and relaxation modulus

The method of approximation previously used for creep or relaxation individually must not be misinterpreted, because it is obvious that $E(p)$ and $D(p)$ are related In fact, combining (2 16) and (2 20) shows that $E(p)D(p) = 1$ Hence, using (2 18) and (2 21), one finds

$$E(p)D(p) = p^2\bar{D}_{c\,p}(p)\bar{E}_{el}(p) = 1 \tag{2 45}$$

so that if $\bar{E}_{1}(p)$ is specified, e g , as through (2 36), then $\bar{D}_{c\,p}(p)$ is uniquely determined from (2 45), and vice versa if $\bar{D}_{c\,p}(p)$ is prescribed Specifically, multiplication of the respective transforms of (2 34) and (2 42) requires

$$\left[E_g - \int_0^\infty \frac{H(\tau)d\tau}{p\tau + 1}\right]\left[D_g + \int_0^\infty \frac{L(\tau)d\tau}{p\tau + 1}\right] = 1 \tag{2 46}$$

On the other hand, as the modified power laws for both creep and relaxation are approximations, the resolution of relative accuracy should properly rest upon experimental evidence

Comparison of typical data (Fig 4) for a viscoelastic carboxy terminated polymer, commercially produced as unfilled HC rubber, reflects the fact that the time-dependent relaxation modulus and creep compliance are essentially reciprocal throughout the time range, not only at the limit values, i e , $D_{c\,p}(t) = [E_{el}(t)]^{-1}$ It should be emphasized, however, that, accurately, the reciprocity exists only in the transform plane, e g , Eq (2 45), but that, if necessary for engineering expediency, the reciprocity can be tentatively extended on an ad hoc basis For comparative purposes, the modified power law fit to the relaxation modulus for a filled HC propellant, as given by Kruse,[13] is reproduced in Fig 5

Interrelation with the dynamic data

It is frequently necessary to convert from relaxation data to dynamic data For this purpose, it is convenient to transform (2 34), namely,

$$\bar{\sigma}(p) = \left\{E + \int_0^\infty \frac{H(\tau)d\tau}{[p + (1/\tau)]\tau}\, p\right\} \bar{\epsilon}(p) \tag{2 47}$$

and, upon noting (2 26) with $p = i\omega$, to find

$$E^*(\omega) \equiv E'(\omega)\, iE''(\omega) = E_e + \int_0^\infty \frac{H(\tau)}{i\omega + (1/\tau)} \frac{i\omega}{\tau} d\tau \tag{2 48}$$

which gives the real and imaginary parts

$$E'(\omega) = E + \int_0^\infty \frac{H(\tau)\omega^2\tau^2}{1 + \omega^2\tau^2} \frac{d\tau}{\tau} \tag{2 49}$$

$$E''(\omega) = \int_0^\infty \frac{H(\tau)\omega\tau}{1 + \omega^2\tau^2} \frac{d\tau}{\tau} \tag{2 50}$$

It would be desirable at this point to insert, for example, the modified power law (2 41) and integrate explicitly This latter step does not yield a simple result, but, as a related approximation, Catsiff and Tobolsky[14] show that the difference between $E_{rel}(t)$ and $E'[(\omega) = 1/t]$ is very small, with the result that, as long as $-1 < n < 2$,

$$E'(\omega) = E_{el}(1/\omega) + [(\pi/2)\csc(n\pi/2) - \Gamma(n)]H(1/\omega) \tag{2 51}$$

where

$$H(\tau) = c\tau^{-n} \tag{2 52}$$

is the straight (unmodified) power law approximation to the relaxation spectrum valid only through the transition region The complex modulus, with a similar assumption for $H(\tau)$, becomes

$$E''(\omega) = [(\pi/2)\sec(n\pi/2)]H(1/\omega) \qquad -1 < n < 1 \tag{2 53}$$

These formulas and others have been collected and discussed by Smith,[15] who also compared the accuracies of the various approximations against published experimental data for polyisobutylene

Series approximation

Having now some idea of methods for characterizing the material behavior through any of four types of tests, it is appropriate to consider how the information will be used in stress analysis Assuming, therefore, that experiments have been performed at, say, constant strain rate, fitted numerically to a linear differential operator or modified power law, and, perhaps, subsequently converted to relaxation modulus, creep compliance, or dynamic form, it is desirous to record also the transformed operator $E(p)$ For-

mally, having obtained $E_{el}(t)$, for example, one can determine $\bar{E}_{r\,1}(p)$ as

$$\bar{E}_{el}(p) = \int_0^\infty E_{rel}(t) \exp(-pt)dt \qquad (2\,54)$$

and then $E(p) = p\bar{E}_{el}(p)$ Alternatively, a knowledge of the material constants a_n, b_n permits $E(p)$ to be written down formally as the ratio of two polynomials It develops, however, that either procedure leads to numerical complexity when $E(p)$ is incorporated into the stress analysis; indeed, insertion of even the simple modified power law representation (2 39) into (2 54) leads to a complicated transform in terms of incomplete beta functions [10] It is desirable, therefore, to have some method of representation which is not only accurate but tractable

In attacking this problem Schapery[4] has taken advantage of the decaying exponential character of viscoelastic deformations to propose an effective collocation scheme Choosing the relaxation modulus for illustration, he assumes that

$$E_{el}(t) = E_e + \Sigma E_k \exp(-t/\tau_k) \qquad (2\,55)$$

which Dirichlet or Prony[82] series expansion can be thought of as an arbitrary expansion of the function $E_{el}(t)$ into a "Fourier series" of real exponentials having the Fourier coefficients E_k and modulus (i/τ_k) instead of the usual integer k Under certain conditions, this expansion is mathematically complete, although it is not possible to write down explicitly the solution for the coefficients as in usual Fourier analysis Schapery then selects N decades of time over the transition range of the experimental data and sets the range of τ_k such that one τ_k falls in each decade over this range He proceeds to collocate N points against the experimental data and observes that, for vanishingly small times, the glassy modulus must be recovered, namely,

$$E_{el}(0) = E_g = E + \sum_i^n E_k \qquad (2\,56)$$

so that the collocation is performed at $N-1$ points

Reading the values of $E_{el}(t_j)$ at the $N-1$ points, t_j leads to a set of linear algebraic equations from which to determine the E_k Schapery points out the important fact that this matrix is essentially triangular and can be solved easily by simple means (slide rule or desk calculator), even when the transition range extends over 20 decades Moreover, it is also important that the Laplace transform of (2 55) is straightforward:

$$\bar{E}_{el}(p) = \frac{E}{p} + \Sigma \frac{E_k}{p + (1/\tau_k)} \qquad (2\,57)$$

or

$$E(p) = p\bar{E}_{rel}(p) = E_e + \Sigma \frac{p\tau_k E_k}{p\tau_k + 1} \qquad (2\,58)$$

and essentially permits the factorization of the ratio of the two polynominals (2 7) in an expeditious fashion It further may be noted that the spectrum of retardation times is distributed over the transition range at the discrete real values τ_k

Furthermore, with $p = i\omega$, the complex modulus also can be computed easily:

$$E^*(\omega) = E'(\omega) + iE''(\omega) = E_e + \Sigma \frac{i\omega_k\tau_k E_k}{i\omega_k\tau_k + 1} \qquad (2\,59)$$

such that

$$E'(\omega) = E_e + \Sigma \frac{E_k\omega^2\tau_k^2}{1 + \omega^2\tau_k^2} \qquad (2\,60)$$

$$E''(\omega) = \Sigma \frac{E_k\omega\tau_k}{1 + \omega^2\tau_k^2} \qquad (2\,61)$$

Also, the tensile stress during a constant strain-rate test is easily found by integrating (2 24) using (2 55):

$$\sigma_{t\,n}(t) = E\,Rt + \Sigma E_k R\tau_k[1 - \exp(-t/\tau_k)] \qquad (2\,62)$$

so that it is readily seen that a knowledge of the E_k over a finite number of decades of time associating the range of τ_k with the transition range readily permits alternate representations of the data after the E_k have been determined once, as in a relaxation test An illustrative example of the Schapery inversion is given in the Appendix

To complete this aspect of the material representation, one should next show how $D_{c\,p}(t)$ could be obtained from the curve fit of $E_{el}(t)$ As mentioned earlier, the mathematically correct way of determining $D_{c\,p}(t)$ is through the Laplace transform relation (2 45) Thus, one would compute

$$\bar{D}_{c\,p}(p) = [p^2\bar{E}_{\,1}(p)]^{-1} = \left[p^2\left\{\frac{E_e}{p} + \Sigma \frac{E_k\tau_k}{p\tau_k + 1}\right\}\right]^{-1} \qquad (2\,63)$$

and formally invert using

$$D_{c\,p}(t) = \frac{1}{2\pi i}\oint \bar{D}_{\,p}(p) \exp(pt)dp \qquad (2\,64)$$

On the other hand, one could, following (2 55), assume

$$D_{\,p}(t) = D_g + \Sigma D_k[1 - \exp(-t/\tau_k)] \qquad (2\,65)$$

with the limit requirement for the rubbery compliance at $t \to \infty$,

$$D_{crp}(\infty) = D_g + \Sigma D_k = D_e \qquad (2\,66)$$

and compute the transform

$$\bar{D}_{c\,p}(p) = \frac{D_g + \Sigma D_k}{p} - \Sigma D_k\left(p + \frac{1}{\tau_k}\right)^{-1} = \frac{D_e}{p} - \Sigma \frac{D_k\tau_k}{p\tau_k + 1} \qquad (2\,67)$$

With $[p^2\bar{E}_{\,1}(p)]^{-1}$ a known function of p, collocate (2 63) as a function of p to find the D_k Knauss[16] has carried through this process for an HC rubber and found that the results are nearly indistinguishable from those obtained much more directly using the simple ad hoc relation (Fig 4b)

$$D_{c\,p}(t) \doteq [1/E_{el}(t)] \qquad (2\,68)$$

which can then be collocated in the physical time plane to determine the specific values of D_k in (2 65) With these values thus determined, the components of the complex compliance $D'(\omega)$ and $D''(\omega)$ can be computed in an analogous manner to that used in finding $E'(\omega)$ and $E''(\omega)$ from $E_{\,1}(t)$ as in (2 60) and (2 61)

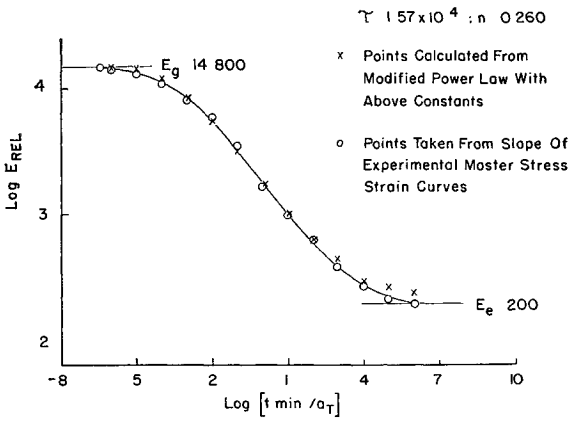

Fig 5 Modified power law representation of relaxation modulus for HC propellant ($a_T = 1$ at $T = -30°C$) [13]

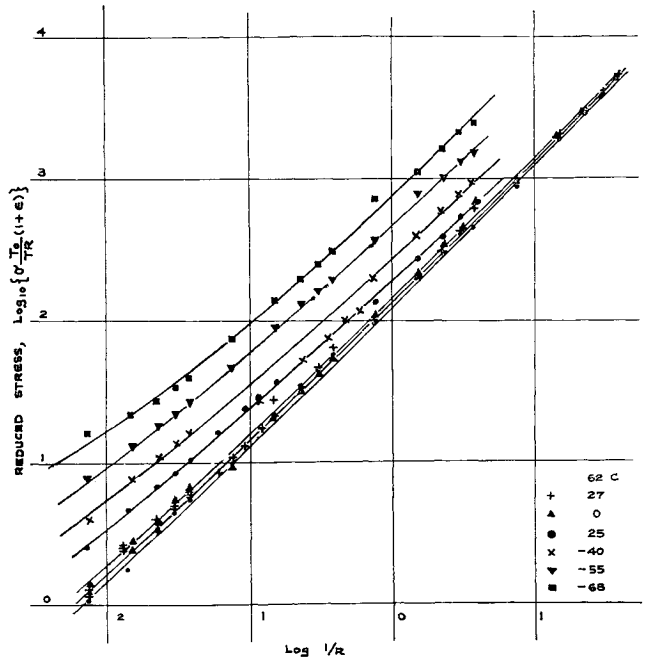

Fig 6 Stress-strain curves from constant strain-rate test at different temperatures; unfilled HC rubber [16]

Time-Temperature Shift

So far, little has been said of the effect that temperature has upon the constitutive equation It has developed, however, that there exists a fortunate, although essentially unexplained, association between time and temperature which reflects quantitatively the observation that behavior at high temperatures and high strain rates is similar to that at low temperatures and low strain rates The usual form of this interrelation, due to Williams, Landel, and Ferry,[17] is

$$\log_{10} a_T(T) \equiv \log(t/t_R) = -K_1(T - T_R)/[K + (T - T_R)] \tag{2 69}$$

where t is the physical time to observe some phenomenon at the temperature T (°K) compared to the time for a similar phenomenon at a reference temperature T_R For most unfilled elastomeric systems, it has been found experimentally that $K_1 = 8\,86$ and $K = 101\,6$ By multiplying numerator and denominator by the constant rate R, $a_T = \epsilon_T/\epsilon_0$, so that, under constant strain-rate conditions, (2 69) can be interpreted as relating strains at two different temperatures

Using this time-temperature relation, or the Williams, Landel, and Ferry (WLF) equation, one can, therefore, deal simply in terms of a reduced or reference time*

$$\xi = t_R = t/a_T(T) = tA(T) \tag{2 70}$$

which is independent of temperature Materials that follow this law are classed as thermorheologically simple The definition of a reduced time for varying transient temperature is given by

$$t_R = \int_0^t \frac{du}{a_T[T(u)]} \tag{2 71}$$

which is seen to reduce to (2 70) for isothermal conditions

To understand the implications of (2 70), consider the Dirichlet series (2 55), which can represent the relaxation of a discrete model in uniaxial tension,

$$E_{\mathrm{rel}}(t) = E_e + \Sigma E_k \exp(-t/\tau_k) \tag{2 72}$$

If one neglects the linear dependence of the spring or non-flow segments upon absolute temperature because of the relatively small percentage effect over the temperature ranges of usual concern for elastomers,† that is, $E(T/T_R) \doteq E$, and, hence, assumes that all of the characteristic relaxation times τ_k depend upon temperature in the manner (2 70), i e ,

$$\tau_k = \tau_{kR} a_T \tag{2 73}$$

then (2 72) becomes

$$E_{\mathrm{rel}}(t) = E + \Sigma E_k \exp\left(-\frac{t}{a_T \tau_{kR}}\right) = E + \Sigma E_k \exp\left(-\frac{t_R}{\tau_{kR}}\right) \tag{2 74}$$

It is obvious that there will be no change in the relaxation modulus with temperature, provided that the physical times are all divided by the temperature shift factor

The term shift factor arises from the way in which a_T is determined experimentally By way of illustration, if stress relaxation due to constant-strain input is measured at various temperatures over the usual four or five decades of time of which most constant rate testing machines are capable and the resulting data are plotted on log-log paper, they might look as in Fig 6 It would appear that if one held the upper cold temperature curve fixed and translated the lower curves to the right by an increasing amount, depending upon the temperature, a continuous smooth curve would result from the "temperature shift" One would then have constructed a table or plotted a graph of the decades of temperature shift from the reference low temperature as a function of temperature This graph, in the form of $\log a_T$ (ordinate) vs T (Fig 7), is called the shift curve and is the one which is usually well approximated by the WLF expression (2 69), except at the warmer temperatures in this polymer It should be noted that the reference temperature in (2 69), which is normally 50°K above the glass temperature of the elastomer, is consistent with the −80°C glass temperature for HC binder It also should be remarked that the WLF relation also seems to apply to filled polymers, although Milloway and Wiegand[18] have presented some evidence that a vertical, as well as a horizontal, shift may be necessary for best accuracy

The fact that this scheme works so well for polymeric materials suggests that there is something rather simple in the nature of flow processes of polymer molecules It was first shown by Leaderman, Smith, and Jones[19] that the solution viscosity of polymer molecules above a certain minimum chain length is independent of chain length and dependent only upon temperature Second, it was shown by Rouse and Sittel[20] that the distribution of relaxation times governing solution viscosity is strictly a function of chain-length distribution Zimm[21] then extended these statements to bulk viscosity It follows, therefore, that a given relaxation time τ_k, characteristic of any one element of a mechanical model or of the kth flow segment in a polymer chain, must depend separately upon temperature and chain length as postulated in (2 73)

A complete discussion of the mechanics of the shifting procedure, with expository background material, has been presented by Smith[22] and Landel and Smith [23]

3 Engineering Analysis

As intimated earlier, the facility with which one can carry out a viscoelastic analysis depends to a large extent upon the correspondence rule by which an elasticity problem is associated with the viscoelastic one In its earliest form, it was first proposed by Alfrey[3] and extended by Tsien[24] and

* The various common notations are combined here for later use

† Nevertheless, it is customary to plot normalized modulus and stress data vs reduced strain rate as ET_R/T or $\sigma T_R/T$ vs t/a_T

Lee,[25] as well as being explored for the anisotropic case by Biot [26] The technique hinges essentially upon transforming the equilibrium, compatibility, and boundary conditions with respect to time in order to obtain a new set of "elasticity" equations in the transform plane The transform variable p is then merely a parameter during the solution of the associated problem The final step requires the inversion of the transform solution back into real time

Because the effectiveness of the method depends essentially upon the existence of a transform, as a practical matter, the technique is restricted to linear viscoelasticity Furthermore, there are certain problems within this class which must be treated differently One of these is that where the boundary conditions change in a nonproportional way with time, as in a rolling contact problem,[27] or when the physical boundary itself changes with time [28 29] Another important class is that of transient thermoviscoelastic problems, of which more will be said later Nevertheless, a significant number of practical problems can be treated using the correspondence principle Typical illustrations, chosen primarily from those occurring in the analysis of solid rocket motors, will now be given

The first example presented earlier[1] relates to a pressurized thick-walled cylinder Consider, therefore, the following formal steps for obtaining the viscoelastic stresses, strains, and displacements in an infinitely long (plane strain) thick-walled tubular cylinder of viscoelastic material encased in a thin elastic shell Let the assembly be subjected to a varying internal pressure $P(t)$

1) Assuming that the material is elastic, write down the elastic solution for σ_{ij}, ϵ_{ij}, and u_i as a function of the geometry, loading, and elastic materials, e g , $\epsilon_{ij} = \epsilon_{ij}(x_k;\ P,\ E,\ \nu)$

2) Replace all time-varying quantities by their Laplace transform equivalents:

$$\sigma_{ij}(t) \rightarrow \bar{\sigma}_{ij}(p) \qquad \epsilon_{ij}(t) \rightarrow \bar{\epsilon}_{ij}(p)$$

$$u_i(t) \rightarrow \bar{u}_i(p) \qquad P(t) \rightarrow \bar{P}(p)$$

3) Replace the elastic constants by their viscoelastic equivalents:

$$K \rightarrow K(p) \qquad G \rightarrow G(p)$$

$$E \rightarrow E(p) \qquad \nu \rightarrow \nu(p)$$

These replaced values are obtained from the material characterization either as the ratio of polynomials (2 7) and (2 8) or as the transformed Dirichlet series (2 58)

4) Transform the physical boundary conditions, e g ,

$\sigma_{ij}(t),\ u_i(t)$ to $\bar{\sigma}_{ij}(p),\ \bar{u}_i(p)$

5) Solve the associated elasticity problem, now formulated in terms of the transformed field equations and boundary conditions for the transformed stresses, strains, and displacements to obtain, e g ,

$$\bar{\epsilon}_{ij} = \bar{\epsilon}_{ij}[x_k;\ P(p),\ E(p),\ \nu(p)]$$

6) Carry out the inversion of the dependent variables, e g ,

$$\epsilon_{ij}(x_k,t) = \mathfrak{L}^{-1}[\bar{\epsilon}_{ij}[x_k,p)]$$

For the problem at hand we have the internal and external radii a and b, respectively, with the pertinent equations:

Equilibrium

$$\frac{\partial \sigma}{\partial r} + \frac{\sigma_r - \sigma_\theta}{r} = 0 \tag{3 1}$$

Compatibility

$$\nabla^2(\sigma_r + \sigma_\theta) = 0 \tag{3 2}$$

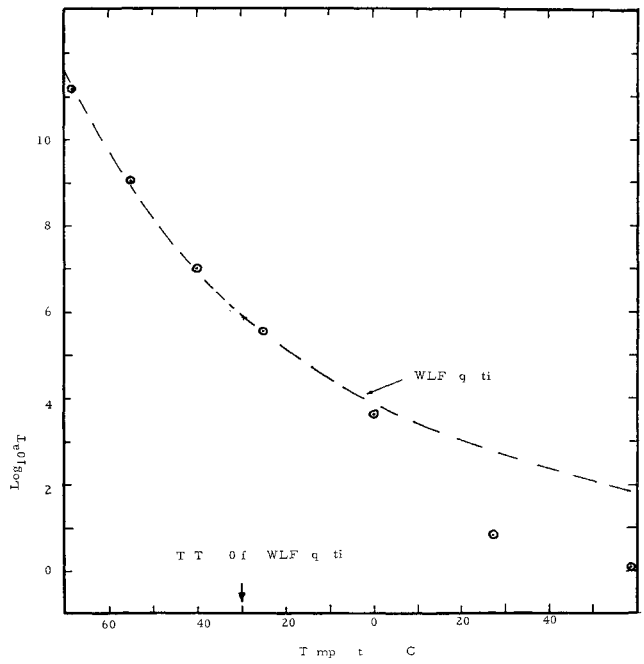

Fig 7 Shift factor for reduction of stress-strain data of Fig 6

Boundary Conditions

$$\sigma\ (a) = 0 \tag{3 3}$$

$$u(b) = u\ (b) \tag{3 4}$$

$$\sigma\ (b) = \sigma\ (b) \tag{3 5}$$

where the subscript c refers to the case of properties E , ν_c, and thickness h

Observing the first rule, the elastic solution can be easily obtained For example, the contact pressure $\sigma\ (b)$ between the case and grain is

$$\sigma\ (b) = \frac{2(1 - \nu)a^2P}{[a^2 + (1 - 2\nu)b^2] + \dfrac{(b^2 - a^2)(1 - \nu_c^2)bE}{(1 + \nu)hE}} \tag{3 6}$$

and the associated elastic solution becomes, therefore,

$$\bar{\sigma}\ (b,p) = \frac{2[1 - \nu(p)]a^2\,\bar{P}(p)}{a^2 + [1 - 2\nu(p)]b^2 + \{(b^2 - a^2)(1 - \nu^2)bE(p)/[1 + \nu(p)]hE\}} \tag{3 7}$$

For given loading and material properties, the solution for $\sigma\ (b,t)$ can be formally obtained by direct inversion

It is at this point that computational difficulties develop because, in a discrete element model for $E(p)$ and $\nu(p)$, each of which involves a ratio of two polynomials, it is readily seen that when the fractions are cleared it does not take many terms in $E(p)$ or $\nu(p)$ to generate large-term polynomial ratios for $\bar{\sigma}\ (b,p)$ The complexity, of course, arises in factoring the polynomials in order to compute the inverse transform For this reason, anything more than a four- or five-element representation of the material becomes unwieldy On the other hand, if one is seeking only qualitative viscoelastic results, a small element approximation may be sufficient

In the earlier paper,[1] for example, the result for a step pressure $P = p_i$, $\bar{P}(p) = p_i/p$ and an incompressible body $\nu = \frac{1}{2}$ was based upon a two-element Voigt representation for the tensile modulus

$$\sigma(t) = 3\left[\eta\frac{d\epsilon(t)}{dt} + G_0\epsilon(t)\right] = 3G_0\left[\tau\frac{d}{dt} + 1\right]\epsilon(t) \tag{3 8}$$

such that

$$E(p) = [\bar{\sigma}(p)/\bar{\epsilon}(p)] = 3G_0(p\tau + 1) \quad (3\ 9)$$

With this substitution and $\lambda \equiv b/a$, (3 7) becomes

$$\bar{\sigma}_r(b,p) = \frac{p_i}{p} \frac{1}{1 + 2(1 - \nu^2)(\lambda^2 - 1)(bG_0/hE)(p\tau + 1)} \quad (3\ 10)$$

which can be easily inverted using transform tables to find

$$\sigma(b,t) = \frac{p_i}{1 + 2(1 - \nu^2)(\lambda^2 - 1)(bG_0/hE)} \times \left[1 - \exp\left(\frac{-\{1 + 2(1 - \nu_c^2)(\lambda^2 - 1)(bG_0/hE)(t/\tau)\}}{2(1 - \nu^2)(\lambda^2 - 1)(bG_0/hE)}\right)\right] \quad (3\ 11)$$

wherein it may be noted that, at long times, the solution approaches the elastic one Note incidentally that, for a rigid case, the relative rigidity bG_0/hE approaches zero The stress state tends to hydrostatic compression (with zero strain) as would be expected in an incompressible rigidly enclosed configuration

The purpose of this example has been to illustrate the mechanics of the correspondence rule, but it becomes evident that, if realistic material properties are used, the computations could become unwieldy For this reason, and following the technique he applied to material characterization, Schapery[4] has proposed two approximate transform inversions that can be used for an arbitrary, and, hence, a realistic, measured material characterization Although others have dealt with the same problem,[30] the advantages of the Schapery inversions are their essential simplicity and potential with respect to increased accuracy

The first of these he has called the direct method It is useful in estimating the viscoelastic response to a step input and is related to the well-known qualitative association between the Laplace transform parameter p and physical time t, namely, that short time corresponds to large p and long time to small p Specifically, his result, illustrated by the previous problem, gives

$$\sigma(b,t) \doteq (p\bar{\sigma}_r(b,p))_{p=1/2t} \quad (3\ 12)$$

where the factor 2 is the quantitative factor introduced into the previously noted qualitative association It arises because of minimizing the error in the approximation for functions that vary rather slowly as a function of p The inversion formula does not depend specifically upon the material characterization aside from the slow variation with the parameter p and, hence, is independent of any particular model representation As actually used, one prepares a table or graph of $E(p)$, and $\nu(p)$ if the experimental data are available, as transformed from the Dirichlet series (2 55) into (2 58) with p considered real Then, for the step function input, the response $\bar{\sigma}_r(b,p)$ is computed also as a function of p, having inserted the appropriate values of $E(p)$ and $\nu(p)$ for the point p in question The result is plotted vs p on the abscissa and the scale relabelled $(2t)^{-1}$ and finally replotted vs t In the foregoing problem, for example,

$$\left.\frac{\sigma(b,t)}{p_i}\right|_{\text{step}} = \left[\frac{2[1 - \nu(p)]}{1 + [1 - 2\nu(p)]\lambda^2 + \{(\lambda^2 - 1)(1 - \nu_c^2)bE(p)/[1 + \nu(p)]hE\}}\right]_{p=1/2t} \quad (3\ 13)$$

which is not restricted to a small-element, discrete model approximation of the material properties The viscoelastic response to an arbitrary input $P(t)$ rather than the simple step is calculated using the Duhamel integral, namely,

$$\sigma(b,t) = \int_0^\infty \sigma(b,\tau)|_{\text{st p}} \left[\frac{\partial P(t - \tau)}{\partial \tau}\right] d\tau \quad (3\ 14)$$

which requires repeated, usually numerical, integrations that, however, are not unduly tedious Indeed, depending upon the nature of $P(t)$, a Dirichlet collocation to $\sigma(b,t)$ can often be multiplied into an analytical form of the pressure derivative, and the general response obtained by quadrature

The second of the Schapery inversions can be applied directly to an arbitrary input, and, while requiring more work, permits circumventing the Duhamel integration, if other than the result to a simple step is required Indeed, this second collocation method, identical to that used in fitting the material property data, has been applied successfully by Williams and Arenz[31–33] in comparing analytical and experimental photoviscoelastic responses for stress wave propagation in a viscoelastic bar Illustrating this method, again with the pressure problem, one anticipates that the physical response will be expressible in a Dirichlet series with unknown coefficients

$$\sigma(b,t) = \gamma_0 + \Sigma\, \gamma_k \exp(-t/\tau_k) \quad (3\ 15)$$

which in the transformed representation

$$\bar{\sigma}(b,p) = \frac{\gamma_0}{p} + \Sigma \frac{\gamma_k}{p + 1/\tau_k} \quad (3\ 16)$$

is collocated to (3 7) wherein the transform of the desired general pressure input $P(p)$ is incorporated Once the γ_k are determined in the p collocation, the desired answer is immediately available from (3 15)

The collocation procedure is illustrated in the Appendix, along with the results for a typical pressure problem, wherein actual material properties are used and approximated by both a discrete element model and the collocation representation

Other Loading

The same technique can be used to calculate the viscoelastic response for other loading conditions A typical loading for solid rocket motors would be that due to inertia, either a 1-g environmental storage loading for long times or a high-g acceleration loading for short times ‡ From the elastic standpoint, the solution is identical except for the magnitude of the acceleration From the viscoelastic one, however, the rocket would respond according to the density of the relaxation spectrum in either the long or short time range For inertia loadings the designer is usually interested in two quantities: 1) the magnitude of the slump deformations which tends to reduce or increase the port diameter with a consequent effect upon the burning time and thrust curve, and 2) the magnitude of the shear-out stress at the grain-case interface as, for example, during a highly accelerated boost phase This design problem is complicated by several important factors that influence the stress analysis One of these is the change in buckling stress due to the viscoelastic core This particular problem has been reviewed by Zak and Williams,[34] who have included a bibliography of the effect of elastic core stabilization, and some comments and preliminary estimates on the effect of viscoelasticity The general influence of such a core is, of course, stabilizing, but more quantitative evaluations of the magnitude would possibly permit the designer to take advantage of this strengthening influence

Important geometric quantities affecting the stresses and slump deformations are the diameter ratio b/a and fineness ratio L/D of the rocket and whether the ends of the tubular grain are supported or free The first computation

‡ An alternate direction solution is sometimes possible, as in the case of an ablating, longitudinally accelerating rocket [33]

one would make is that for plane strain,[10] but efficiency in design dictates that one assess the changes in the infinitely long (plane strain) stress, strain, or deformation results due to b/a or L/D It develops that a three-dimensional elastic stress analysis is required So far, the analytical solution has not been obtained in a useful form, although formally it can be developed following the basic solution given by Pickett [35] The solution is further complicated by the existence of (elastic) stress singularities at the ends of the grain which have been identified with those of plane strain by Zak [36] The net result is that numerical solutions requiring extensive digital programming have been required This important need was finally met by Parr and Gillis,[7] who have presented a fairly complete set of parametric design charts as a function of b/a, L/D, and ν for stresses, strains, and displacements in a tubular grain for axial inertia loadings as well as for pressure and steady-state thermal conditions § Recently, Messner[8] has also been working upon this problem with a more general program to extend the Parr and Gillis results for the flat-ended grain to those with ogival heads His results have also been of value for the failure analysis of a "poker-chip" specimen, of which more will be said later, in the limit case of $L/D \to 0$

In many situations where an elastic case is employed, it is sufficient to assume that the effective case rigidity is infinite, i e , $bE/hE \to 0$ One situation where this is not true is the lateral inertia condition for a tubular grain, such as its environmental condition of lying on its side As in the axial position, the solution for a rigid case is straightforward,[37] [38] but for an elastic case in the horizontal position the most comprehensive reference is that of Gillis [39] The bending rigidity of the case in this position is so weak that the viscoelastic core may reach unduly large strains and deformations

Another environmental loading of particular interest is that of vibration, with some fundamental work for cylinders being contributed by Baltrukonis [40] The natural frequency of a system is proportional to the elastic modulus, and it is evident that if the modulus is time dependent then the natural frequency would change with time also Tormey and Britton[9] have recently shown the results of vibrating some viscoelastic specimens at their natural frequency and, among other things, have been able to trace the actual resulting flow as due to the heat dissipated during the vibration If, for purposes of illustration, one neglects inertia effects in, say, a longitudinal vibrating bar, one can show that the strain lags the stress by an amount proportional to the imaginary part of the complex modulus Indeed, the viscous dissipation energy loss per cycle is

$$W_d' = \pi\sigma_0\epsilon_0 \sin[\tan^{-1}\{E''(\omega)/E'(\omega)\}] \qquad (3\ 17)$$

which is zero at the limiting low and high frequencies but has an intermediate maximum If all of this energy were converted into heat, and no allowances were made for radiation or conduction away from the specimen, the temperature rise per cycle would be $\Delta T' = W_d'/(\rho c)$, which for representative viscoelastic materials would be of the order

$$\Delta T_F \approx 0\ 006\ W_d'(\text{in-lb/in}^3) \qquad (3\ 18)$$

leading to relatively high temperatures in relatively few cycles The more detailed analysis is relatively straightforward but is again tedious for a particular material [41]

The final loading to be discussed is that due to temperature It is convenient to divide the thermal problems into three areas: 1) determination of the temperature distribution, 2) steady-state analysis, and 3) transient analysis For the common situations, a stress calculation is predicated upon the knowledge of temperature as a function of space and time For reasonable geometries, it is even possible to solve the heat-conduction equation exactly, as in slabs or cylinders Unfortunately, the solutions for the temperature, although exact, are frequently in infinite series form, which analytically complicates the problem Consider, for example, $a_T[T(x,t)]$, which is basically an exponential variation in the ratio of two terms containing the temperature (2 69), each of which is nominally an infinite series Such complicated dependence, particularly when a_T itself is to be manipulated upon, is not conducive to easy analytical interpretation As one alternative, Seward[42] has exploited the use of Biot's variational technique[43] [44] to obtain tractable simple transient temperature expressions for rocket grains For the degree of engineering accuracy desired in most problems, this approach, or perhaps a Galerkin approximation,[44] is recommended

Steady-state temperature analysis, in many cases, can be replaced by equivalent boundary loadings, and this fact has been used particularly for tubular solid rocket grains and even those containing star perforations [45] [46] Because the coefficients of expansion in the grain and case are in the ratio of 10:1, a steady-state change in temperature imposes a calculable interface pressure at $r = b$ on the thick walled cylinder Such problems, therefore, are basically isothermal problems in both space and time The next most complicated problems are those for which the temperature is timewise constant but allowed to vary with the space dimension This situation may occur such that the outside of the geometry is at one temperature and the inside at another This problem is equivalent to a common problem in stress analysis wherein the material is assumed to be temperature but not rate dependent In boilers, for example, there will be a temperature variation through the wall thickness requiring, if accurate answers are desired, the incorporation of $E = E[T(x)] = E(x)$ into the solution This type of problem was discussed several years ago by Hilton [47] As the material properties are not time dependent, there is no interaction with the viscoelastic time-dependent deformations, and the Laplace transformation technique is still valid

As to transient analysis, there are two types The first of these is for problems in which the temperature changes with time only and not with the spacial variable Here an analysis can be conducted for certain cases by performing the Laplace transformation with respect to reduced time (2 70) The second, which is more difficult but simultaneously more interesting because completely satisfactory techniques have not been obtained, is the general one wherein the temperature varies with both space and time Before reviewing the salient features of transient thermoviscoelastic analysis, it is perhaps worth restating the qualitative description of the time regimes of interest [2] Obviously, if the heat conduction is infinitely slow, all of the viscous dashpots will have time to relax independent of heat conduction, and we have the case where effectively $T = T(x)$ only On the other hand, if the heat conduction is infinitely fast and the temperature change immediately stabilizes to steady state, the same $T = T(x)$ only situation holds as far as viscoelastic analysis is concerned The difficult problem then occurs when the two diffusion processes of temperature variation and viscoelastic deformation are changing at essentially the same rate The dimensionless parameter is revealed qualitatively by considering dominant or representative terms in the temperature expansion

$$T \sim \exp(\kappa t_H/l^2) \qquad (3\ 19)$$

and in the viscoelastic relaxation

$$u \sim \exp(t/a_T\tau) \qquad (3\ 20)$$

§ By considering plane strain conditions, but for a star rather than tubular cross section, they have shown that the governing equations for an axially accelerated rigid case configuration reduce to $\Delta^2 w(r,\theta) = \rho g/G$, with $w(b) = 0$ and $\partial w/\partial n = 0$ on the inner boundary Solution of this equation permits an evaluation of stress concentration effects during longitudinal inertia See Rohm and Haas Quarterly Progress Report on Engineering Research, no P-62 27 (January 1963)

so that dimensionally the important ratio is[2]

$$t/t_H = \kappa a_T \tau/l^2 \tag{3 21}$$

such that, for the diffusivity κ, zero or infinite, the dimensionless parameter does not enter, but where $\kappa \approx l^2/a_T\tau$, one must anticipate a transient analysis Note also that this parameter does not change linearly with the characteristic length In general, and particularly for combined loadings, it will be impossible to make direct scaling experiments relating small specimens to large ones insofar as their transient thermoviscoelastic behavior is concerned

Morland and Lee[5] have formulated the transient thermal problem for a linear viscoelastic medium For completeness, it is worth exhibiting their equations and showing how they differ from the isothermal ones Recalling, therefore, that the (point) stress-strain relation actually depends upon the reduced time (2 70), which in the general thermal situation $T(x,t)$, is defined through (2 71), using the Morland-Lee notation

$$\xi(x,t) = \int_0^t A[T(x,u)]du \tag{3 22}$$

one can, upon selecting the linear differential form¶ (2 5) and (2 6), write the stress-strain law for variable temperature as

$$[a_n'\partial^n/\partial\xi^n + \quad + a_0'] s_{ij}(x_k,\xi) = [b_m'\partial^m/\partial\xi^m + \quad + b_0'] e_{ij}(x_k,\xi) \tag{3 23}$$

$$[c'\partial/\partial\xi + \quad + c_0'] \sigma_{ii}(x_k,\xi) = [d'\partial/\partial\xi^s + \quad + d_0'] \epsilon_{ii}(x_k,\xi) \tag{3 24}$$

The equations of equilibrium without body force at a fixed physical time are

$$\left.\frac{\partial \sigma_{ij}(x_k,t)}{\partial x_j}\right|_t = 0 \tag{3 25}$$

It is readily apparent, without even considering the compatibility equations, that the dependent variables are not expressed in terms of the same independent variables In order to do so, one must either convert (3 23) and (3 24) to an (x_k,t) dependence, or else convert (3 25) to an (x_k,ξ) dependence

In the first alternative one may use (3 22) to write

$$\left.\frac{\partial}{\partial t}\right|_x = \left.\frac{\partial}{\partial \xi}\right|_x \left.\frac{\partial \xi}{\partial t}\right|_x = a_T[T(x,t)] \left.\frac{\partial}{\partial \xi}\right|_x \tag{3 26}$$

which leads to variable $f(x,t)$ coefficients in the linear differential operator forms (3 23) and (3 24), for which normal transform techniques are not defined As the other alternative, one can convert (3 25) to a reduced time functional dependence by considering $\sigma_{ij}(x_k,t) = \sigma_{ij}(x_k,\xi)$ and writing (3 25) so as to obtain

$$\left.\frac{\partial \sigma_{ij}}{\partial x_j}\right|_\xi + \left.\frac{\partial \sigma_{ij}}{\partial \xi}\right|_x \left.\frac{\partial \xi}{\partial x_j}\right|_t = 0 \tag{3 27}$$

in which case the equation no longer has the usual form of the elasticity equilibrium equations

Sets of (3 23, 3 24, and 3 27), or alternatively (3 23) and (3 24), with derivative substitutions of (3 26) and (3 25), are then internally consistent, but none are convenient, and they lead to considerable difficulty in engineering applications Only a few restricted problems have been solved Morland and Lee were able to obtain some mathematical solutions assuming somewhat unrealistic combined mechanical and thermal incompressibility, but Muki and Sternberg[48] extended the work by solving the specialized slab and sphere geometries In the slab problem, general thermorheologically simple shear and bulk behavior was assumed, but for the spherical case, the additional restriction of elastic bulk response was introduced It may be noted, incidentally, that Schapery[4] compared his shorter approximate inversions to both the asymptotic solution and the Lee and Rogers[30] finite difference solution of the Muki-Sternberg integrals with excellent results

Hilton and Russell[49] have proposed an extension to Alfrey's theorem for transient analysis essentially using incremental steps in time They consider a viscoelastic problem having a constant temperature over a small time increment $t_i - t_{i-1}$, compute the state at the end of the interval t_i, and use it as the initial state for the next time interval $t_{i+1} - t_i$ over which the temperature has a new constant value In application, however, this latter procedure becomes somewhat involved, as found by Valanis and Lianis,[50] who have used essentially the same approach, as well as introducing another interesting feature by iterating the solution in terms of the compressibility, beginning with zero bulk compliance ($K = \infty$)

In conclusion it may be said that, with the exception of the transient thermal problem for which additional "reduction to practice" work is recommended, convenient methods are available for an engineering analysis of linearly viscoelastic media, provided that the material properties are prescribed In this connection, it is interesting to note that this characterization, in a gross sense, hinges upon only five unknowns if a modified power law approximation to the relaxation modulus can be invoked These are the glassy and rubbery moduli E_g and E, the slope through the transition region n, the characteristic relaxation time τ_0, and the glass temperature of the material $T_g = T_R - 50°C$ Indeed, for preliminary design purposes, it proves convenient to collect and tabulate various viscoelastic materials characterized in this simple way With these five parameters the relaxation curve can be drawn, fit with a Dirichlet series using the Schapery collocation, interconverted to alternate representations, and analytically transformed easily to the transform plane for the stress analysis Finally, the transformed stress quantities also can be back-collocated with the transformed Dirichlet series to obtain the time dependent stresses, strains, or displacements

4 Failure Criteria

The last of the three categories to be discussed relates to failure criteria for viscoelastic media Whereas the previous section was mainly concerned with investigating methods of estimating the stresses or strains due to prescribed applied loads, we now turn to a consideration of predicting the maximum imposed loading at which either excessive deformation or a fracture threshold is reached

By way of illustration in solid rockets, these two characteristic types of failure are exemplified by slump due to inertia and grain cracking due to pressurization Generally, the first of these is tied in rather closely with ballistic performance and storage procedures, that is to say, a maximum permissible deformation without fracture is more or less arbitrarily prescribed If this is the case, it becomes a relatively simple matter to complete the analysis by applying the viscoelastic analysis technique previously developed to calculate the loading or time corresponding to that state when this critical deformation is reached As the procedure is straightforward, although not necessarily simple in a given problem because the strain analysis itself can be complicated, no additional remarks upon the deformation criterion will be made

On the other hand, the prediction of a fracture threshold is considerably more difficult, because, in general, it will depend

¶ It should be noted that it is possible to express the stress-strain relations equally well in terms of integral relations, e g ,

$$s_{ij}(x,\xi) = \int_0^\infty G(\xi - \xi') \left[\frac{\partial e_{ij}(x,\xi')}{d\xi}\right] d\xi'$$

upon the state of multiaxial stress, and sufficient experimental data have not yet been accumulated to give a final criterion Also, because of the time or rate dependence in viscoelastic bodies, one could justifiably presume that fracture would depend upon the strain rate history Further analysis, therefore, is rather handicapped by the present state of the art in which the bulk of the testing has been carried out at constant strain rate to failure in uniaxial specimens Some of the recent results in enlarging this area of endeavor since the last survey[3] and the review by Wiegand[51] of mechanical properties evaluation will be summarized based in large part on the report of Lindsey et al [52] dealing with triaxial failure

By way of introduction, however, it is appropriate to include some typical uniaxial failure data as points of reference (Fig 8) These data are customarily determined by measuring the applied force during constant crosshead travel at rates in the range 10^{-2}–10^{2} in /min at temperatures between −60° and 160°F Precision is hampered by the lack of an adequate, convenient, and automated local strain-measuring device for the potentially large strains involved As a matter of expediency this has led to deducing stress based usually on an initial cross-sectional area, although some investigators use deformed area assuming incompressibility and the use of an effective gage length to calculate strains This latter difficulty arises mainly from the filletted-end of the JANAF test specimen which, because of viscoelasticity, permits the material to flow out of the gripping device Although benchmarks and optical means have been used to smoe extent to obtain increased accuracy, the fact that data must be recorded for various strain rates leaves this particulai matter as still a definite problem area ** Nevertheless, Fig 8 shows typical data obtained at different temperatures, as shifted with the a_T factor (Fig 7) It is thus the analog to ANC allowable data for metals, but including also the parameters of time and temperature

Referring to Figs 7 and 8, note that the stress data (based on original area) have been normalized by a temperature ratio because polymer theory predicts a linear increase of retractive forces with absolute temperature Both sets of data were normalized using the temperature shift factor, experimentally deduced from separately shifting the stress-strain values as measured in a constant strain-rate test The WLF curve fits reasonably well for a reference temperature $T_R = 243°K$

Before passing on to a consideration of fracture under multiaxial load conditions, it should be observed that the temperature shift correlation is reasonably well founded experimentally, but that the limited strain-rate capability of the Instron tester is not particularly well suited for verifying the correlation over wide extremes This may be noted in Fig 8, where the test data at various temperatures barely overlap One would feel much more confident if, for example, the open circle (100°C) data, obtained over the $1/Ra_T$ range 1 to 4, could be extended to lower values by increasing the strain rate, and hence lower $1/Ra_T$ at the same 100°C temperature Bearing in mind, however, the limitation of the tester, approximately 20 in /min cross head motion maximum, it is impossible to fulfill this desire without changing the specimen, which would not be particularly acceptable

The obvious answer is to inquire if higher rate testers would be available Several have been developed One of these is the Allegheny Instrument Company device,[56] which is

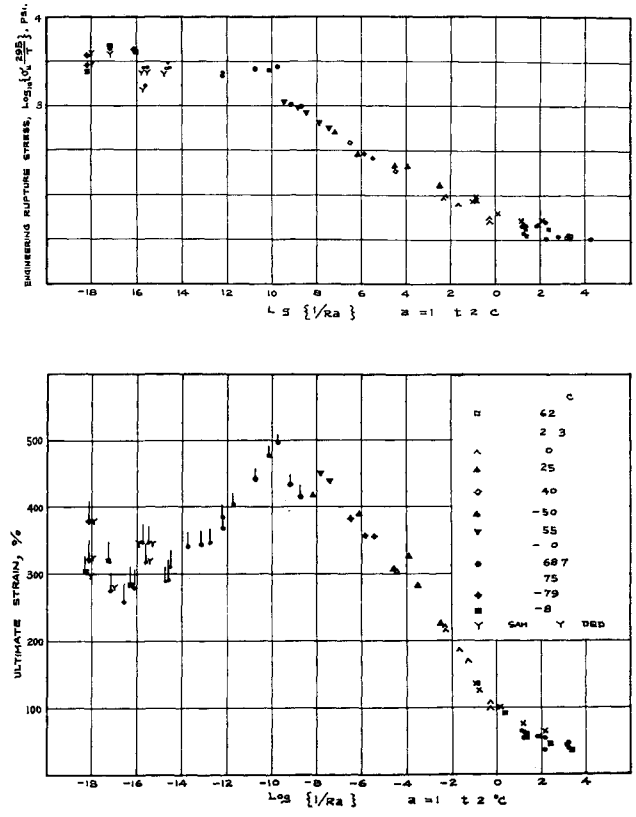

Fig 8 Ultimate stress and strain in a constant strain-rate test; unfilled HC rubber [16]

generally well known Another is one developed by E I DuPont de Nemours and described in a recent paper by Jones [57] Basically, this latter machine, which achieves high loading rates by means of a controlled explosion of smokeless powder in the head, can strain JANAF specimens up to approximately 200,000 in /min Although it is premature to generalize, indications from this and other high-speed tester work are that the theoretical WLF shift factor for ultimate fracture of tensile JANAF specimens is sufficiently valid for engineering purposes

Failure Surface

In general, materials may be subjected to six stress components, three normal and three shearing, which can be resolved into three principal stresses On the other hand it is usually simplest to test under one-dimensional condition such as tension It is legitimate to ask the following question: Having measured the strength in one combination of the three stresses ($\sigma_1 = \sigma_2 = 0$; $\sigma_3 = \sigma_{ult}$), can one then predict without further tests the failure under some other arbitrary combination of the three stresses? Obviously, following a postulated failure criterion, crucial experiments are required to prove or disprove the criterion Previous experience with metals has indicated that there is no universal criterion for all materials, although considerable progress has been made Over the years, several proposed theories of failure have been advanced Nadai[58] enumerates, for example, several different failure criteria, primarily as used in the study of metals Each criterion defines some particular function of the stress field or strain field, the value of which is to be determined empirically, because molecular theories of strength are not advanced to the point of calculating such limits theoretically When the appropriate function is exceeded, the associated yield, rupture, or fracture takes place Seven such criteria are as follows: 1) the maximum principal stress; 2) the maximum principal strain; 3) the maximum principal stress difference (or shear stress);

** It may be noted that Baldwin and Cooper[53] and Jones[54] have had some success in using a square, flat-end, bonded specimen that reduces the flow near the grips and, hence, removes part of the gage length indeterminacy Greensmith[55] has reported and reviewed another type of tensile test wherein ring or thin hoop specimens are stretched over the two Instron testing machine supports Except for a very small length curved directly around the end supports, the entire double length of the link specimen is in tension Gage length uncertainty is minimized, and the specimen is easy to test, although somewhat harder to prepare, particularly for filled materials

Table 1 Various possibilities in the different octants

Octant	1	2	3	Number of positive stresses
I	+	+	+	3
II	+	+	−	2
III	+	−	+	2
IV	+	−	−	1
V	−	+	+	2
VI	−	+	−	1
VII	−	−	+	1
VIII	−	−	−	0

4) the maximum principal strain difference (or shear strain); 5) the maximum total strain energy; 6) the maximum distortional strain energy; and 7) the maximum conserved distortional strain energy

The important point to note is that no universal fracture criterion has been established, and that the success of a given fracture hypothesis depends in large measure upon the material with which it is associated

Because of the many criteria for fracture, it is convenient to have a method that permits the analyst to visualize their region of possible application Inasmuch as the three principal stresses are orthogonal and participate in all stress theories of failure, one way of presenting the criteria is in terms of principal stress space where the magnitudes of σ_1, σ_2, and σ_3 are measured along the orthogonal axes to form octants A similar approach could be adopted for strains The rupture of an uniaxial tensile specimen at the stress σ_3* would, therefore, correspond to a point on the σ_3 axis at the particular value σ_3* Other combined loadings would, in a similar manner, correspond to other points on a rupture surface $F(\sigma_1,\sigma_2,\sigma_3) = \text{const}$, where the object of failure testing would be to perform experiments under all different combinations of combined stresses in order to trace out the failure surface in all octants Presumably there would be many surfaces, each corresponding to a given strain rate for which the surface was obtained Then, having obtained such surfaces experimentally, the analyst would proceed to check out various criteria in the different octants, and the one lying closest to the test surface would be the desired failure criterion

It is convenient to tabulate in Table 1 the various possibilities in the different octants by simple permutation By virtue of equivalence of the three principal axes, it is noted that there are four categories of octants characterized by the number of stresses of the same sign Thus octants II, III, and V are similar, and octants IV, VI, and VII are similar This means that, for an isotropic material, only four octants need to be tested If, in addition, it is known that the compressive properties are the same as the tensile properties, then only two octants need to be tested On the other hand, if the material is anisotropic or if anisotropy is induced by virtue of straining, then it will be necessary to check six octants for an orthotropic material and eight for a completely aeolotropic material

If, therefore, we were to assume isotropy, a reasonable degree of complication over the simple uniaxial specimen would be to design experiments with stress or strain combinations of +++, ++−, +−−, and −−− or even, for engineering expedience, to assume similar behavior in tension and compression,†† thus restricting immediate consideration to +++ and ++− The first of these latter two combinations implies triaxial tension, and the second mixed tension-compression, as in a pressure vessel with hoop and axial tension and radial compression Each of these two octants possesses, of course, certain limit cases, including the plane ++0 separating them, which corresponds to the biaxial tension in a stretched drumhead We shall, therefore, restrict our main attention to stress or strain combinations lying within the quarter space or its limit planes, and the tests designed to determine failure within it

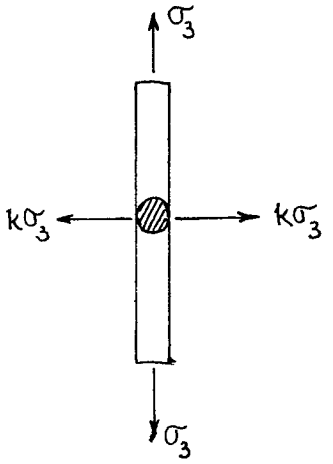

Fig 9 Geometry for a pressurized tensile specimen

Pressurized tensile test

The uniaxial failure stress data (+00) for a given strain rate can be plotted on all three coordinate axes, and will be dismissed without further comment In filling out other octants, again recalling the working hypothesis that tension and compression effects may be interchanged, one of the simplest extensions of the present uniaxial tensile test using the Instron tester is to enclose the specimen in a leak-proof container filled with air or liquid maintained at an arbitrary compressive pressure With the same criticisms of the basic test with no external pressure, a triaxial tension-compression stress field can be imposed Suppose that the geometry is as shown in Fig 9 Then the stress and strain analysis for the central portion of the specimen subjected to the uniaxial tensile stress gives

$$\sigma_3 = \sigma \qquad \epsilon_3 = \sigma_3/E[1 - 2\nu k] \tag{4 1}$$

$$\sigma_1 = \sigma_2 = k\sigma \qquad \epsilon_1 = \epsilon_2 = \sigma_3/E[-\nu + (1 - \nu)k] \tag{4 2}$$

One would expect, therefore, an apparent uniaxial modulus for this triaxial field of

$$E_a = E/(1 - 2\nu k) \tag{4 3}$$

where, because in the tests as described k is negative corresponding to a compressive stress, the apparent modulus would be smaller than the uniaxial modulus

Some unpublished data of Kruse[59] suggest that, for a filled material, the failure under these conditions agrees equally well with failure data in uniaxial tension expressed either as octahedral shearing stress or uniaxial ultimate tensile strain

Diametral compression of a disk

Fitzgerald[60] has suggested that the disk-type specimen also may be used in an alternate manner to examine a mixed tension-compression biaxial stress field If a circular disk of uniform thickness h is loaded in diametral compression by a load P, the stresses at the center are of opposite sign and equal to[61] (see Fig 10)

$$\sigma_x(0,0) = P/\pi bh \tag{4 4}$$

$$\sigma_y(0,0) = -(3P/\pi bh) \tag{4 5}$$

Furthermore, the diametral extension $2u(b,0)$ along the

†† As a practical matter it may be noted that the main objection to this premise, especially for filled materials, is the "pull-away" effect between filler particles and the binder which occurs preferentially in tension It is this fact that prevents a single failure criterion from applying to all octants

horizontal ($y = 0$) plane is

$$2u(b,0) = [P/Eh][(4/\pi) - 1 + \nu] \qquad (4\,6)$$

Provided that there is no local failure at the point of load application, this specimen has the advantage that the critical stresses occur at the center and may be easily observed Furthermore, measurements of the horizontal extension permit an indirect check on the accuracy of the foregoing formulas Presumably, as long as the extension stays linear with the applied load, even though the deformations near the point of application may be large, one would feel justified in using these stress formulas based upon infinitesimal deformation theory From the standpoint of fracture, Fitzgerald[60] has found that the character of failure at the center changes from tensile to shear depending upon the temperature of the test This latter point, of course, emphasizes its potential significance as a sensitive test for determining a fracture criterion

Incidentally, it may be observed in passing that the range of central stresses which can be imposed, i e , $\sigma_y/\sigma_x = -3$ from the preceding equations, could be extended by the use of elliptical instead of circular specimens, although at some expense in experimental simplicity The results of a combined theoretical and experimental investigation using the elliptical specimens have been reported by Brisbane [62]

Hollow tube tests

Provided that a satisfactory strain measurement is available, the behavior of an internally pressurized thin- or thick-walled cylinder up to and including burst would yield fracture information under biaxial tension, for zero axial stress, or with the added triaxiality, depending upon the nature of a finite longitudinal stress This type of specimen was first used with mixed success at the U S Naval Ordnance Test Station[63] employing an oil for the pressurization The major difficulties, aside from such obvious ones as preventing leakage, are to obtain an accurate strain history and to measure the applied time-varying pressure These tests can be used upon either thin- or thick-walled cylinders, and with or without being enclosed in a case In some cases it will be more convenient to check out a thin case-bonded design using externally mounted wire strain gages and inferring the tube strains by working backward using the theoretical solution For most purposes, however, the resultant case-to-grain stiffness is so high that accuracy is poor

It also should be mentioned that it may be practicable to combine torsion with the pressurization of thin-walled hollow cylinders for which situation the theoretical solution is known Another test variation using the hollow tube is to examine the orthotropic behavior of multilayered cylinders

Biaxial failure in sheet specimens

Failure experiments under biaxial tension, which contribute data for the limiting planes of octant I of the failure surface, can be most easily performed using a pressurized membrane On the other hand, even a thin membrane has finite thickness, and, hence, in trying to resist bending, particularly near the supporting edge, the specimen often tends to fracture under combined bending and stretching stresses [64 65] Also, the contribution to the stress field due to the clamping pressure at the support, necessary to prevent the specimen from pulling out of the test fixture when the pressure is applied, tends to make the correlation of analysis and experiment difficult On the other hand, if the failure takes place near the center of the, say, circular membrane specimen (incidentally, usually implying rounding off the support edges in order to induce failure away from the edge), useful data should result if the applied strain rate can be controlled

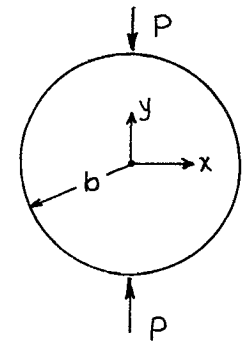

Fig 10 The diametral compression test [60]

Homogeneous biaxial test

Another type of biaxial test is one wherein equal biaxial tension has been imposed, without normal pressure, by merely applying uniform displacement around the edges of a square sheet specimen whose sides are glued to wire hooks approximately $\frac{1}{2}$ in apart [66] The other ends of these hooks are attached to small ball bearings that are supported and are allowed to slide on two V-shaped guides that can be seen in Fig 11 As the load is applied to the guides this arrangement produces the homogeneous biaxial extensions described previously There is, of course always some nonhomogeneous deformation of the specimen near the edges; however, by painting square grids on the surface and observing their deformation, it was found that these edge effects propagated only a small distance into the specimen The biggest problem with these tests is the premature fracture in the vicinity of the hooks This problem was eventually solved by changing the design and spacing of the hooks

Strip tension test

A second biaxial, but not equal, tensile field specimen tested at Graduate Aeronautical Laboratory of the California Institute of Technology[66 67] consisted of a rectangular sheet specimen bonded on its longer edges to steel plates, which are then connected to the testing machine grips (Fig 12) A tensile stress σ is applied perpendicular to the longer edges of the specimen The stress normal to the sheet σ_y is zero Under these conditions, a major portion of the specimen between the plates is subject to plane strain conditions along most of its longer length, i e , $\epsilon_x = 0$, $\epsilon_y = \nu\epsilon$, $\epsilon = \sigma(1 - \nu^2)/E$ Near the ends, of course, the conditions are not plane strain; however, the end effects can be reduced by increasing the length of the specimen

The latter two tests have proved reasonably efficient for assessing both the mechanical characterization and the failure characteristics of several materials such as[66–68] the following: SBR-1500 rubber (1 75% S); 2) SBR-1500 rubber (3% S); 3) Polyurethane foam rubber (47% voids by volume, 40 μ diam); 4) natural rubber (2% sulfur); 5) natural rubber (4% sulfur); 6) CIS-4; 7) Paracril-B; 8) Neoprene-GNA; and 9) Butyl-217

The large strain characterization of the material has been approached by first determining an appropriate strain energy function [69] Evaluation of the failure data and the subsequent determination of a failure criterion from the experimental data is described in Ref 70 For these foam materials, it was tentatively established that the failure criterion was the mean hydrostatic stress Thus, the first octant failure surface for the foam would be a plane cutting the three principal stress axes at the uniaxial failure stress, or, more generally

$$\sigma_{\text{c iti al}} = \sigma_{\text{uni xial}} = (\tfrac{1}{3})[\sigma_1 + \sigma_2 + \sigma_3] \qquad (4\,7)$$

It would be premature, of course, to assume that the same criterion would hold in general, but, in principle, this ex-

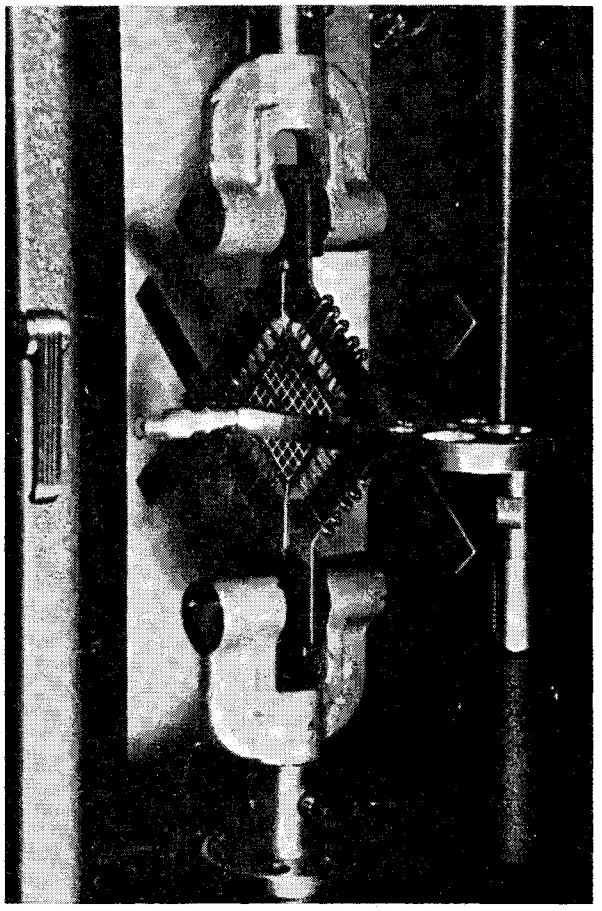

Fig 11 Homogeneous biaxial tension

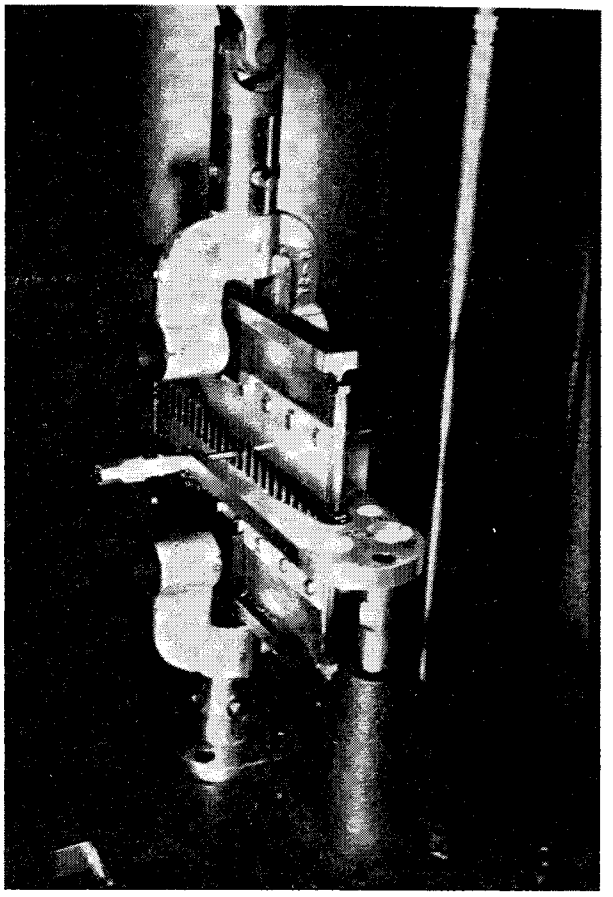

Fig 12 Strip biaxial tension

ample serves to illustrate the direction which further correlation will take for the solid viscoelastic rubber specimens

Triaxial tension failure

It previously has been indicated that one of the important combined stress fields is that of triaxial tension Fracture under this loading condition, octant I, would contribute heavily toward determining the over-all fracture surface In particular, if the material could be considered as isotropic and homogeneous, thus probably excluding filled materials, a definition of the failure surface in this octant would give one-fourth of the information necessary for defining the complete surface because, as shown earlier, only four of the eight octants would be independent

The production of a triaxial tension field is not easy unless only small stresses are desired, in which case vacuum pressure can be used Usually, however, fracture stresses exceed 15 psi, and one must resort to more complicated means of producing the desired triaxial condition A commonly proposed method is that of a thin disk cemented between two relatively rigid platens that are pulled in tension The dimensions of the specimen give rise to its designation as a "poker-chip" test Fortunately, since the material to be tested is rather soft compared to the easily available and much harder platen materials,‡‡ the softer disk sandwiched between the harder bars will be restrained because of its thinness from its usual contraction perpendicular to the load and, hence, will generate a triaxial tension stress field

The elementary analysis for this case may be made by assuming the disk infinitely thin such that the external radius is sufficiently far from the center to assume that the only nonzero displacement w is in the x_3 axial direction Under these conditions, one is led to deduce for small deformations

$$\sigma_3 = \sigma \qquad \epsilon_3 = \frac{\sigma(1 - 2\nu)(1 + \nu)}{E(1 - \nu)} \tag{4 8}$$

$$\sigma_1 = \sigma_2 = [\nu/(1 - \nu)]\sigma \qquad \epsilon_1 = \epsilon_2 = 0 \tag{4 9}$$

so that the apparent axial modulus becomes

$$E_a = E\left[\frac{1 - \nu}{(1 - 2\nu)(1 + \nu)}\right] \tag{4 10}$$

where it may be noted that for rubbery materials that are characteristically nearly incompressible, i e , $\nu = \frac{1}{2}$, the triaxial tension approaches hydrostatic with a consequent infinite apparent axial stiffness

When a finite radial size of a poker-chip specimen is considered, analytical difficulties arise, as discussed more fully in the basic reference [52] In this reference, however, a fairly accurate approximate solution is given which compares very well with a numerical one programmed by Messner,[8] except for the edges where the previously mentioned stress singularities occur Considering the thinness of the specimen, all stresses are averaged through the thickness and, upon assuming displacement functions that satisfy the displacement boundary conditions at $z = \pm 1$ in a specimen of radius a,

$$-u(r\,z) = (1 - z^2)g(r) \tag{4 11}$$

$$w(r,z) = \epsilon_0 z \tag{4 12}$$

where the applied strain is ϵ_0, and u and w are the radial and axial displacements, respectively, the averaged equations of equilibrium are found to be satisfied if

$$g''(r) + (1/r)g'(r) - [(1/r^2) + M]g(r) = 0 \tag{4 13}$$

Elementary analysis leads to a computation for the triaxial

‡‡ Note that it would not be practical to test steel for its triaxial tensile behavior in this manner

stress field in the specimen For example, the apparent modulus of the specimen $E_A \equiv \sigma_z$ (average)$/\epsilon_0$ was found to be

$$\frac{E_A}{E} = \frac{3\nu}{1+\nu}\ \frac{K}{E}\left[1 - \frac{2I_1(aM^{1/2})}{aM^{1/2}I_0(aM^{1/2})}\right] + \frac{1}{1+\nu} \times \left\{1 + \frac{2I_1(aM^{1/2})\left[1 - \frac{I_1(aM^{1/2})}{aM^{1/2}I_0(aM^{1/2})}\right]}{aM^{1/2}I_0(aM^{1/2})\left[1 + \frac{1-2\nu}{\nu}\left(1 - \frac{I(aM^{1/2})}{aM^{1/2}I_0(aM^{1/2})}\right)\right]}\right\} \quad (4\ 14)$$

where

$$M \equiv 3(1-2\nu)/[2(1-\nu)] = 3\mu/(\lambda + 2\mu) \quad (4\ 15)$$

This apparent modulus can be conveniently employed for determination of the bulk modulus of a nearly incompressible material Given the aspect ratio a and the experimentally measured modulus E_A, the modulus ratio E/K can be deduced from a graph of (4 14) This plot is shown in Fig 13, where it is observed that E_A/Ea^2 depends only upon the parameter $[a(E/K)^{1/2}]$ for $a \geq 30$ Also shown on the figure are the early approximate results of Gent and Lindley [71]

The triaxial stress distribution at the center of the specimen is also of interest It was found that

$$\frac{\bar{\sigma}(0)}{E\epsilon_0} = \frac{\bar{\sigma}_\theta(0)}{E\epsilon_0} = \frac{3\nu}{1+\nu}\ \frac{K}{E} \times \left\{1 - \frac{1 - (M/3)}{I_0(aM^{1/2}) - [(2M/3)I_1(aM^{1/2})/(aM^{1/2})]}\right\} \quad (4\ 16)$$

$$\frac{\bar{\sigma}(0)}{E\epsilon_0} = \frac{\bar{\sigma}_r(0)}{E\epsilon_0} + \frac{1}{1+\nu} \times \left\{1 + \frac{\nu/2}{(1-\nu)I_0(aM^{1/2}) - [(1-2\nu)I_1(aM^{1/2})/(aM^{1/2})]}\right\} \quad (4\ 17)$$

which yields the triaxial hydrostatic tension field for an incompressible body as in (4 8) and (4 9) It may be mentioned, incidentally, that, for the small strains involved, infinitesimal strain theory is appropriate in contrast to many situations in viscoelasticity where the large deformations require a reassessment of the pertinence of small-strain theory Finally, Fig 14 shows a comparison between this approximate solution and that of Messner [8]

Inasmuch as a failure threshold must be compared with experiments, clear birefringent specimens of Solithane 113 were pulled between Lucite grips (Fig 15) through which the time and location of fracture could be observed, with or without crossed polaroids as desired The object, of course, was to detect the applied load at which the spherical voids first (audibly) popped into sight at the center of the specimen where the local stress could be estimated from (4 16) and (4 17) Instead of resolving the criterion question, a new one was raised: How is the initial flaw or void size, undetectable by microscope or not, related to the local hydrostatic stress field? This question was investigated by formulating a Griffith instability-type criterion, as in crack initiation work, except that provision was made to include large finite strain effects Without amplification of the analysis contained in the reference,[52] the results turn out to depend upon a material parameter $k = 6T/Ea_0$, where T is the usual surface energy, E the elastic modulus, and a_0 the initial flaw size The local stress and extension ratio λ_a at the cavity, as well as the critical hydrostatic tension field p_c at fracture, is given in Fig 16

The unfinished step, now in process at Graduate Aeronautical Laboratory of the California Institute of Technology, is to obtain sufficient data to guarantee the accuracy of the triaxial fracture point as a function of strain rate It may be mentioned also that, in practice, this type of hydrostatic tension field fracture can occur at the interface between the case and solid rocket grain material during cooling A consideration of merely the uniaxial bond strength $\sigma_r(b)$ compared to the uniaxial tensile strength may prove unduly conservative in engineering design

Molecular considerations

Aside from the macroscopic consideration of fracture in terms of over-all stresses and a failure envelope, it must be recognized that fracture first occurs on a microscopic basis, probably along the lines just indicated for cavity formation and growth One of the most convenient methods to study local failure is with specimens containing cracks As an alternative to the observation of small cavities, one can also investigate thin sheet specimens containing central or edge slits, with the added advantage in binder materials of photoelastic obseruations [6] Although this procedure is relatively standard for metals, there has been little emphasis upon extending the same techniques to viscoelastic media The first work was reported by Rivlin and Thomas,[72] who investigated an extension of the Griffith[73] energy instability principle, which led to the determination of a rate- and temperature-dependent energy-dissipation parameter This work and other recent viscoelastic fracture research have been placed in a thermodynamic or energy framework and been reviewed by Williams,[74] who has also included estimates of initial and limiting crack velocity as well as the initiation threshold At the present time it seems fairly well estab

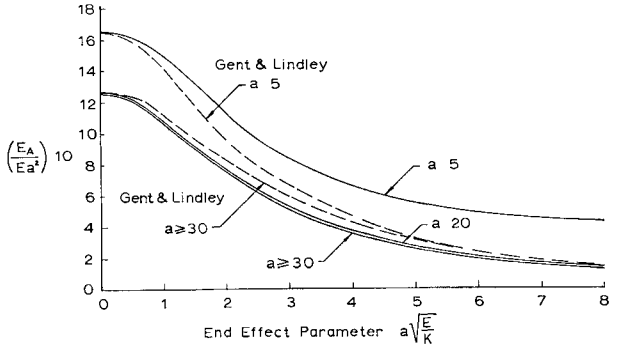

Fig 13 Apparent modulus of disk vs $a(E/K)^{1/2}$ Note: $E/K = 3(1-2\nu)$

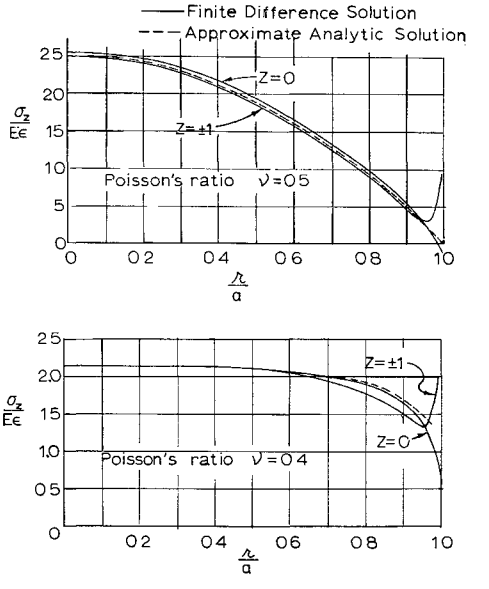

Fig 14 Comparison of axial stresses obtained from two different methods of solution

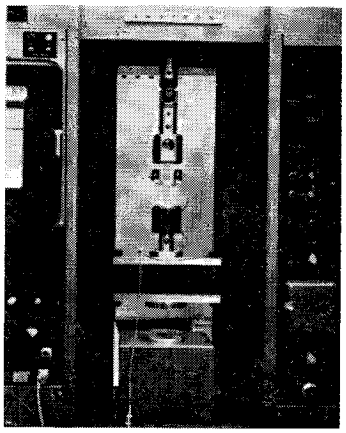

a) Closeup of test specimens and microformers

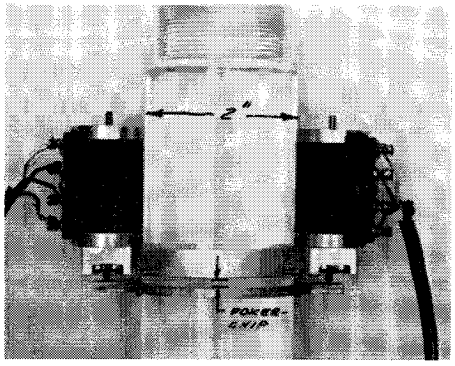

b) Test assembly

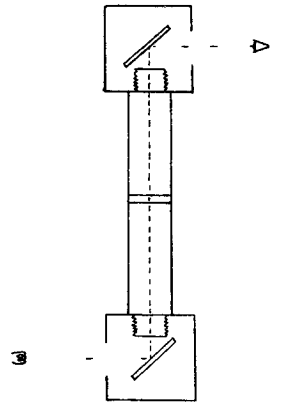

c) Schematic of test assembly

Fig 15 Illustration of poker-chip test [52]

lished that viscoelastic fracture, in contrast to brittle fracture, is limited by viscous dissipation concentrated at the crack tip where the accompanying heat generation simultaneously is degrading the ultimate strength capability of the material

Cumulative Damage

It already has been emphasized that one failure surface is not sufficient, even if defined for all of the octants of principal stress or strain space Because failure is a time- or rate-dependent phenomenon, there would be, in general, one surface for each condition of constant strain rate to failure On the other hand, it is highly unlikely that in a practical situation the strain rate would always remain constant, certainly not if the load were changing with time as is the usual case Hence, one must be able to answer the question posed earlier: Given the constant strain-rate failure data, how can failure under an arbitrary loading and rate history be determined? For the purposes of illustration, it suffices to consider merely a two-step situation If the time to failure is 1 min at 0 1 in /in /min rate, and 0 1 min at 1 in / in /min what is the time to failure if, after 0 5 min at 0 1 in /in /min, the rate is instantaneously changed to a rate of 1 in /in /min? At this point, it is pertinent to recall the hypothesis used by Miner[75] for the fatigue of metals, namely, a cumulative damage law connecting stress level and cycles to failure over M load changes

$$\sum_{i=1}^{M} \left[\frac{N_i}{N_{Ri}}\right]^n = 1 \qquad (4\ 18)$$

where the total life $L = \Sigma N_i$ N_i is the number of cycles at the stress σ_i, and N_{Ri} is the number of cycles to rupture at the stress σ_i In its usual application, the linear form ($n = 1$) is customarily employed Following this same type of approach, Williams[2] suggested that a similar relation might be postulated for polymers whose rate dependence could be associated with cycles §§ Assuming constant temperature for simplicity, or using reduced time, assume

$$\sum_{i=1}^{M} \left[\frac{t_i}{t_{Ri}}\right]^n = 1 \qquad T = \sum_{i=1}^{M} t_i \qquad (4\ 19)$$

where t_i and t_{Ri} are the time the specimen is held at the strain rate R_i and the time to failure at R_i, respectively T is then the total time to rupture over the spectrum of constant strain rates R_i ($i = 1, 2, 3 \quad M$) Assuming a linear relation ($n = 1$), an answer to the previous question is easily found as

$$\frac{0\ 5}{1\ 0}\bigg|_{R=0\ 1} + \frac{t_2}{0\ 1}\bigg|_{R=1} = 1 \qquad (4\ 20)$$

from which $t_2 = 0\ 05$ min, and, hence, $T = 0\ 5 + 0\ 05 = 0\ 55$ min In the integral (linear) form, (4 19) can be replaced by ($n = 1$)

$$\int_0^T \frac{dt(R)}{t_R(R)} = 1 \qquad (4\ 21)$$

which is convenient if the ultimate strain-rate data, Fig 8 replotted as $t_R(Ra_T)$, are fit by an analytical form or if numerical quadrature is performed

The application of (4 19) suffers from many of the same criticisms as (4 18), which, among other things, is that it does not readily distinguish between order of load application In metal applications, Valluri[76] has found an improved fatigue theory dealing with combined microconcepts

§§ An even simpler criterion is the use of average strain rate to failure employed in the ablating accelerating grain problem [83]

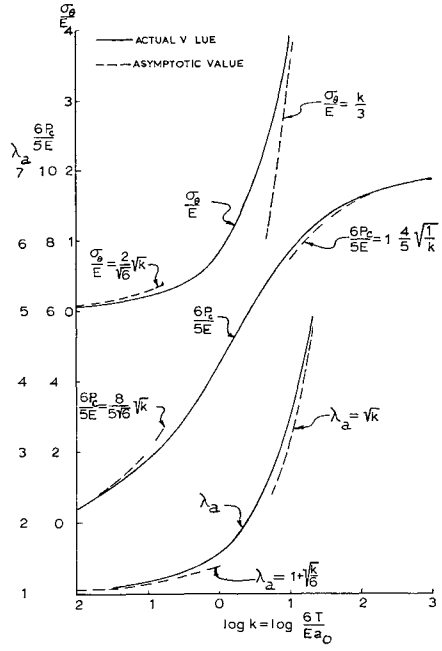

Fig 16 Critical conditions for instability of an initial spherical cavity [52]

and macroconcepts which permits cumulative damage to be evaluated as a natural outgrowth of the development, and predicts that high stresses followed by low lead to shorter life than the reverse ordering In an analogous manner and as an outgrowth of one phase of his work dealing with the micromechanisms of polymer failure, Knauss[6] has been led to some preliminary estimates of damage which also show a sensitivity to ordering Furthermore, some preliminary experimental data tend to substantiate his postulates (Fig 17) Although it is premature to propose general engineering adoption of his line of attack at this time, it appears hope ful that substantial progress can soon be made in evaluating cumulative damage in viscoelastic media

At the present writing, it is impossible to recommend a unique rate-dependent failure criterion As has been indicated, it appears that various quantities are critical depending

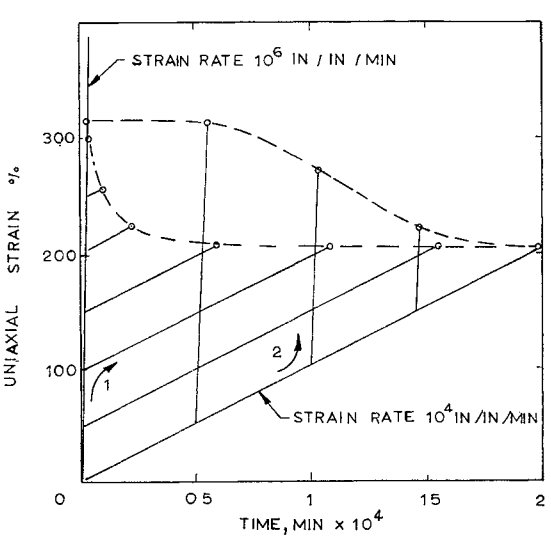

Fig 17 Theoretically predicted effect of loading history upon ultimate strain in a dual strain-rate test [6] Lines denote various traces of strain Example: Arrow 1 indicates sequence of high strain rate to strain of 100%, then low strain rate to rupture Arrow 2 indicates reversed sequence Circles denote calculated rupture points

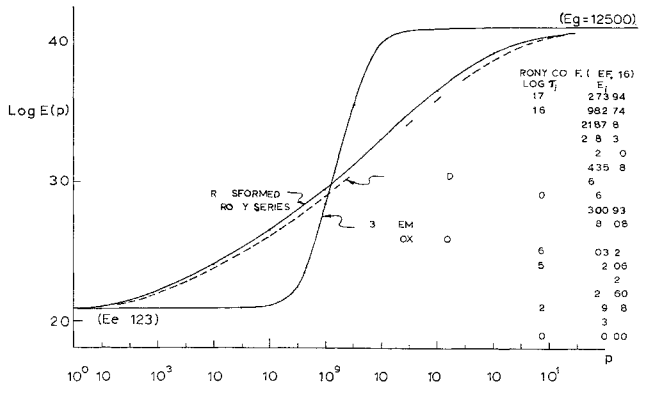

Fig 18 Various transformed modulus representations

upon the material and the stress or strain state for a particular loading The consensus, leavened with engineering judgment, seems to be that uniaxial strain is a reasonable criterion for most situations, such as near star points in grains, but it is obviously incorrect for triaxial stressing of an incompressible material For contact or interface stress conditions, a maximum uniaxial or octahedral stress criterion is believed preferable It is hoped that the results from current research programs now underway at various organizations will soon clarify the present clouded picture

5 Conclusions

Even in this rather lengthy review, it has been impossible to even touch upon many other important contributions to the rapidly expanding subject of viscoelasticity To the extent, however, that the emphasis in this paper has been more toward an integrated discussion of properties, analysis, and failure for direct incorporation in engineering analysis, it is necessary to refer to standard texts such as Stuart[77] or Ferry[78] for more chemically oriented background, and reviews such as Lee's[79] for analytical reinforcement From the engineering standpoint, comprehensive company reports such as those prepared under the direction of Wiegand[80] and Fitzgerald[42 11] are invaluable, and also indicate the gray areas where research and engineering merge

With the forementioned emphasis, it is perhaps worth restating that an engineering structural analysis of viscoelastic materials is both feasible and practical, with the possible exception of transient thermal problems and more definitive multiaxial failure criteria On the other hand, improved techniques for local strain measurements, dynamic testing, and shear-strength evaluation would permit significant and immediate progress

On a philosophical matter, it is the author's conviction that too many engineering stress analysts have shied away from viscoelasticity because the subject and the materials appear different Characteristically, engineers have been trained with metals and ordered metal atomic structure in mind Consequently, when tangled, disordered polymer chains are presented to them, particularly with a lack of adequate chemical, as opposed to metallurgical, background in the behavior of nonmetals, there is a temptation to consider the subject as disordered as the molecular structure

There is certainly an obligation on the part of the schools[81] to begin including certain aspects of nonmetals in the general engineering curriculum, especially because of the many current potential combinations in this day of new, exotic, and mixed-media materials On the other side, however, it is equally true that industry cannot afford to wait for the newly trained talent and must rely upon their current staff But the graduate engineers should not insist upon conducting analyses and solving problems in new areas completely by rule of thumb and engineering judgment They must be

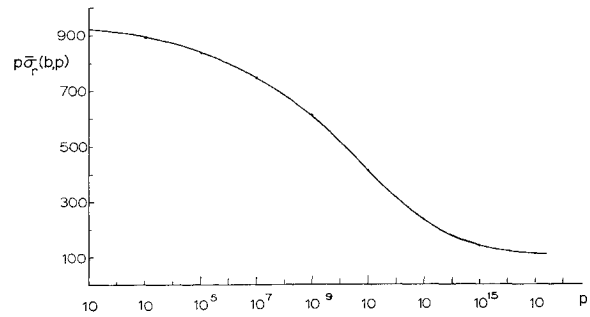

Fig 19 Transformed interface stress using Prony modulus

prepared to invest time in background preparation With the present relative shortage of viscoelastic stress analysts, such an investment can return large dividends

Appendix

To illustrate certain features of a viscoelastic analysis, the interface stress between an elastic case and an incompressible viscoelastic thick-walled cylinder under conditions of plane strain will be calculated for an internal step function in pressure It will be assumed that experimental stress relaxation data have been given as in Fig 4 As the stress analysis requires a knowledge of $E(p) = pE_{el}(p)$, it is first necessary to represent the experimental data

The simplest approximation is to use a three-element model (Fig 1) such as

$$E_{1}^{(1)}(t) = \sigma_{el}(t)/\epsilon_0 = E\{1 + [(E_g/E) - 1]\exp(-t/\tau_m)\}$$

For the experimental data of Fig 4, $E_g = 12{,}500$ and $E = 123$ Fitting the data at the center of the transition region, say E_1 (10^{-10} min) = 1000 psi, it is found that $\tau_m = 0\,377 \times 10^{-10}$ As a more accurate representation, Knauss has fit the data with an 18-point Schapery collocation to the Prony series (2 55)

$$E_{1}^{(2)}(t) = E + \sum_{k=1}^{18} E_k \exp\left(\frac{-t}{\tau_k}\right)$$

For convenience, the curve fit constants are given in the table on Fig 18

These approximations can be transformed, respectively, by direct analytical means to

$$E^{(1)}(p) = pE^{(1)}{}_1(p) = E + (E_g - E)p/(p + \tau_m{}^{-1})$$

$$E^{(2)}(p) = pE^{(2)}{}_1(p) = E_e + \sum_{k=1}^{18} \frac{E_k p\tau_k}{(p\tau_k + 1)}$$

which are compared in Fig 18, along with the approximation

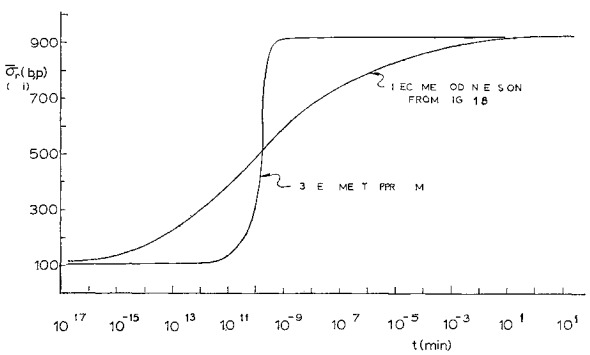

Fig 20 Interface stress due to step function pressurization

resulting from the reflection of $E_{el}(t)$ Note that, if the reflected curve is shifted by one-third of a decade, it nearly coincides with the transformed Prony curve The mathematical reasons for this success are inherently the same as those which support Schapery's direct method of inversion

Proceeding to the solution for the viscoelastic contact stress $\sigma(b,t)$ [Eq (3 6)], as specialized to the incompressible material $\nu = \frac{1}{2}$, one has, for the step function input $P(p) = p_i/p$,

$$\bar{\sigma}(b,p) = \frac{p_i}{p} \frac{1}{1 + 2(\lambda^2 - 1)(1 - \nu^2)bE(p)/3hEc}$$

As a typical example, consider the following specific values of the parameters:

$$E = 1 \times 10^6 \text{ psi} \qquad \lambda = b/a = \tfrac{30}{10} = 3$$

$$\nu = 0\,33 \qquad p_i = 1000 \text{ psi}$$

$$h = 0\,20 \text{ in}$$

so that

$$\bar{\sigma}(b,p) = 10^3/p[1 + 7\,2 \times 10^{-4}E(p)]$$

which is plotted in Fig 19, using the modulus from the Prony series

Using the direct method (3 12), the viscoelastic contact stress is

$$\bar{\sigma}(b,p) = [p\bar{\sigma}(b,p)]_{p=1/2t} = 10^3/[1 + 7\,2 \times 10^{-4}E(1/2t)]$$

By way of comparison, the analytical inversion of the three-element solution gives

$$\sigma(bt,) = 919 - 819\exp(-0\,290\ t/10^{-10})$$

These two solutions are shown in Fig 20, where the poor broad-band quality of the three-element approximation is immediately evident

References

[1] Williams, M L, "The strain analysis of solid propellant rocket grains," J Aerospace Sci **27**, 574 (1960)

[2] Williams, M L, ' Mechanical properties and the design of solid propellant motors," *ARS Progress in Astronautics and Rocketry: Solid Propellant Rocket Research*, edited by Martin Summerfield (Academic Press, New York, 1960), Vol 1, p 67

[3] Alfrey, T, "Non-homogeneous stresses in visco-elastic media," Quart Appl Math **II**, 113–119 (1944)

[4] Schapery, R A, "Approximate methods of transform inversion for viscoelastic stress analysis," Proc Fourth U S Natl Congr Appl Mech **2**, 1075 (1962)

[5] Morland, L W and Lee, E H, ' Stress analysis for linear viscoelastic materials with temperature variation," Trans Soc Rheol **IV**, 233–263 (1960)

[6] Knauss, W G, "Rupture phenomena in viscoelastic materials" Dissertation, California Institute of Technology (June 1963)

[7] Parr, C H and Gillis, G F, "Deformations of case-bonded solid propellant grains under axial and transverse acceleration loads," ARS Paper 2750-63 (January 1963)

[8] Messner, A M, "Stress distributions in poker-chip tensile specimens," Aerojet-General Corp, Tech Paper 127 SRP (September 1963)

[9] Tormey, J F and Britton, S C, "Effect of cyclic loading on solid propellant grain structures," AIAA J **1**, 1763–1770 (1963)

[10] Williams, M L, Blatz, P J, and Schapery, R A, "Fundamental studies relating to systems analysis of solid propellants," Graduate Aeronautical Lab, California Institute of Technology SM 61-5 (February 1961); also Armed Services Technical Information Agency Rept AD 256-905 (1961)

[11] Francis, E C and Cantey, D, ' Structural integrity of propellant grains," Lockheed Propulsion Co Rept 556-F (January 1963)

[12] Elder, A S, communication to the Joint Army-Navy-Air Force (JANAF) Panel on Physical Properties (September

1960); also Goldberg, W and Dean, N W, Ballistic Research Labs Rept 1180 (November 1962)

[13] Kruse, R B, "The role of broad-spectrum mechanical response studies in propellant evaluation," Proceedings 20th Meeting JANAF Physical Properties Panel, Johns Hopkins Univ p 395 (November 1961)

[14] Catsiff, E and Tobolsky, A V, 'Stress relaxation of polyisobutylene in the transition region (1,2),' J Colloid Sci **10**, 375–392 (1955)

[15] Smith, T L, "Approximate equations for interconverting the various mechanical properties of linear viscoelastic materials, Trans Soc Rheol **II**, 131–151 (1958)

[16] Knauss, W G, 'On the mechanical properties of an HC rubber," Graduate Aeronautical Lab California Institute of Technology SM 63-1 (January 1963)

[17] Williams, M L, Landel, R F, and Ferry, J D, "The temperature dependence of relaxation mechanisms in amorphous polymers and other glass-forming liquids," J Am Chem Soc **77**, 3701–3707 (1955)

[18] Milloway, W T and Wiegand, J H., 'Failure criteria for some polyurethane propellants,' Proceedings 20th Meeting JANAF Physical Properties Panel, Johns Hopkins Univ, p 323 (November 1961)

[19] Leaderman, H, Smith, R, and Jones, R, "Rheology of polyisobutylene II Low molecular weight polymers," J Polymer Sci **14**, 47 (1954)

[20] Rouse, P and Sittel, K, Viscoelastic properties of dilute polymer solutions,' J Appl Phys **24**, 690 (1953)

[21] Zimm, B, Dynamics of polymer molecules in dilute solution: viscoelasticity, flow birefringence dielectric loss," J Chem Phys **24**, 269 (1956)

[22] Smith, T L, "Stress-strain-time temperature relationships for polymers," Special Tech Publ 325, American Society for Testing Materials (1962)

[23] Landel, R F and Smith, T L, 'Viscoelastic properties of rubberlike composite propellants and filled elastomers," ARS J **31**, 599–608 (1961)

[24] Tsien, H S, "A generalization of Alfrey's theorem for viscoelastic media, ' Quart Appl Math **VIII**, 104–106 (1950)

[25] Lee, E H, 'Stress analysis in visco elastic bodies," Brown Univ, Div Appl Math, TR 8 (June 1954)

[26] Biot, M A, "Dynamics of viscoelastic anisotropic media," Proceedings 4th Midwestern Conference Solid Mechanics pp 94–108 (September 1955)

[27] Lee, E H and Radok, J R M, "The contact problem for viscoelastic bodies," J Appl Mech **27**, 438–444 (1960)

[28] Radok, J R M and Lee, E H, "Stresses in elastically reinforced, visco-elastic tubes with internal pressure," Brown Univ, Div Appl Math, TR 15 (April 1956)

[29] Arenz, R J and Williams, M L, The stresses in an elastically reinforced pressurized viscoelastic sphere with an eroding boundary," Proceedings 20th Meeting JANAF Physical Properties Panel, Johns Hopkins Univ, p 143 (November 1961)

[30] Lee, E H and Rogers, T G, "Solution of viscoelastic stress analysis problems using measured creep or relaxation functions," J Appl Mech **30**, 127 (March 1963)

[31] Arenz, R J and Williams, M L, Dynamic analysis in visco-elastic media," Proceedings of the Symposium on Structural Dynamics under High Impulse Loading, Dayton, Ohio, Aeronautical Systems Div Tech Doc Rept ASD-TDR-63-140, p 79 (May 1963)

[32] Arenz, R J, ' Uniaxial wave propagation in realistic viscoelastic materials," J Appl Mech **31**, 17 (March 1964)

[33] Arenz, R J, "Theoretical and experimental studies of wave propagation in viscoelastic material," Thesis, California Institute of Technology (1963)

[34] Zak, A R and Williams, M L, "Structural instability of solid propellant rocket motors," NASA TN D-1510 (December 1962)

[35] Pickett, A, "Application of the Fourier method to the solution of certain boundary problems in the theory of elasticity,' J Appl Mech **11**, A-176 (September 1944)

[36] Zak, A R, "Stress singularities in bodies of revolution," J Appl Mech **31**, 150 (March 1964)

[37] Lockett, F J, "Stress analysis of changes of solid-propellant rocket-motors Part I: Effects of vertical storage under gravity and of gas pressure in conduit," Royal Armament Research and Development Establishment, Rept (B) 5/62, Fort Halstead, England (July 1962)

[38] Lockett F J, "Effect of horizontal storage under gravity, ' Royal Armament Research and Development Establishment Rept (B) 7/62, Fort Halstead, England (September 1962)

[39] Gillis, G F, 'Stresses and deformations induced in composite cylinders by transverse body forces," *Proceedings of the First Southeastern Conference on Theoretical and Applied Mechanics* (Plenum Press, New York, to be published)

[40] Baltrukonis, J H, Forced transverse vibrations of a solid, elastic core case-bonded to an infinitely-long, rigid cylinder,' Proceedings 20th Meeting JANAF Physical Properties Panel Johns Hopkins Univ, p 109 (November 1961)

[41] Williams, M L, The axial vibration of a viscoelastic rod,' Graduate Aeronautical Lab California Institute of Technology SM 63-9 (April 1963)

[42] Seward, A L, Thermal grain structural analysis," Lockheed Propulsion Co Rept 577-578-TN-2 (May 1962)

[43] Biot, M A, New methods in heat flow analysis with application to flight structures,' J Aeronaut Sci **24**, 857–873 (1957)

[44] Boley, B A and Weiner, J H, *Theory of Thermal Stresses* (John Wiley and Sons, Inc, New York, 1960), Chap 7

[45] Fourney, M E and Parmerter, R R, Photoelastic design data for pressure stresses in slotted rocket grains, ' AIAA J **1**, 697 (1963)

[46] Williams, M L, ' Some thermal stress design data for rocket grains ARS J **29**, 26 (1959)

[47] Hilton, H H, "Thermal stresses in bodies exhibiting temperature dependent elastic properties," J Appl Mech **19**, 350–354 (1952)

[48] Muki, R and Sternberg, E, 'On transient thermal stresses in viscoelastic materials with temperature-dependent properties,' J Appl Mech **28**, 193–207 (1961)

[49] Hilton, H H and Russell, H G, ' An extension of Alfrey's analogy to thermal stress problems in temperature dependent linear viscoelastic media, J Mech Phys Solids **9**, 152–164 (1961)

[50] Valanis, K C and Lianis, G, 'Studies in stress analysis of viscoelastic solids under non steady temperature, gravitational, and inertial loads,' Purdue Univ, A and E S 62-19 (December 1962)

[51] Wiegand, J H, "Recent advances in mechanical properties evaluation of solid propellants," ARS J **32**, 521–527 (1962)

[52] Lindsey, G H, Schapery, R A, Williams, M L, and Zak, A R, The triaxial tension failure of viscoelastic materials," Aeronautical Research Laboratory ARL 63 152 (September 1963); also Armed Services Technical Information Agency Rept AD 419-128 (September 1963)

[53] Baldwin, J B and Cooper, M H, "Preliminary report on a bonded tensile specimen, Bull 19th Meeting JANAF Physical Properties Panel, Publ PP-13/SPSP-8, p 151 (August 1960)

[54] Jones, J W, Daniel, D, and Johnson, D A, Propellant viscoelastic characterization in creep and stress relaxation tests," Proceedings 20th Meeting JANAF Physical Properties Panel, Johns Hopkins Univ, p 193 (November 1961)

[55] Greensmith, H W, Rupture of rubber VII Effect of rate of extension in tensile tests,' J Appl Polymer Sci **3**, 175 (1960)

[56] Brettschneider, H and Dale, W, Experience with the Alinco high rate tensile tester,' Bull 17th Meeting JANAF Physical Properties Panel, p 43 (May 1958)

[57] Jones, J, Tensile testing of elastomers at ultra high strain rates," High Rate Symposium, Boston, Mass (January 1960)

[58] Nadai, A, *Theory of Flow and Fracture of Solids* (McGraw-Hill Book Co, Inc, New York, 1950), p 175

[59] Kruse, R B, unpublished data, Thiokol Chemical Corp, Huntsville, Ala (March 1962)

[60] Fitzgerald, J E, A biaxial test for solid propellants, ' Bull 19th Meeting JANAF Physical Properties Panel (September 1960)

[61] Timoshenko, S and Goodier, J N, *Theory of Elasticity* (McGraw-Hill Book Co, Inc, New York, 1951), p 107

[62] Brisbane, J J, Stress distribution in an elliptical disk with concentrated loads acting along the axes of symmetry, Quart Rept P-61-25, Rohm and Haas Co (January 1962)

[63] Ordahl, D D, "Burst tests on solid propellants (NOTS burst test),' Bull 8th Meeting JANAF Physical Properties Panel, p 7 (July 1953)

[64] Kruse, R B, unpublished data, Thiokol Chemical Corp, Huntsville, Ala (March 1962)

[65] Spangler R, unpublished data, DuPont Eastern Labs

Gibbstown, N J (September 1961)

[66] Blatz, P J, Ko, W L, and Zak, A R, 'Fundamental studies relating to the mechanical behavior of solid propellants, rocket grains, and rocket motors,'' Graduate Aeronautical Lab California Institute of Technology SM 61-19 (October 1961)

[67] Blatz, P J, Ko, W L, and Zak, A R, "Fundamental studies relating to the mechanical behavior of solid propellants, rocket grains, and rocket motors,'' Graduate Aeronautical Lab, California Institute of Technology SM 61-15 (June 1961)

[68] Blatz, P J, Ko, W L, and Zak, A R, "Fundamental studies relating to the mechanical behavior of solid propellants, rocket grains, and rocket motors,'' Graduate Aeronautical Lab, California Institute of Technology SM 62-27 (November 1962)

[69] Blatz, P J, Ko, W L, and Zak, A R, "Fundamental studies relating to the mechanical behavior of solid propellants, rocket grains, and rocket motors,'' Graduate Aeronautical Lab, California Institute of Technology SM 62-14 (February 1962)

[70] Blatz, P J, Ko, W L, and Zak, A R, "Fundamental studies relating to the mechanical behavior of solid propellants, rocket grains, and rocket motors,'' Graduate Aeronautical Lab, California Institute of Technology SM 62-23 (May 1962)

[71] Gent, A N and Lindley, P B, "The compression of bonded rubber blocks,'' J Brit Rubber Producer's Assoc **173,** 111 (1959)

[72] Rivlin, R S and Thomas, A G, "Rupture of rubber I Characteristic energy for tearing,'' J Polymer Sci **10,** 291 (1953)

[73] Griffith, A A, 'The phenomena of rupture and flow in solids,' Phil Trans Roy Soc (London) **A221,** 163–198 (1921); also "The theory of rupture,'' Proceedings 1st International Congress Applied Mechanics, pp 55–63 (1924)

[74] Williams, M L, "The fracture of viscoelastic material, *Fracture of Solids,* edited by D C Drucker and J J Gilman (Interscience Publishers, Inc, New York, 1963), p 157

[75] Miner, M A, "Cumulative damage in fatigue,'' J Appl Mech **12,** 159–164 (September 1945)

[76] Valluri, S R, "A unified engineering theory of high stress level fatigue,'' Aerospace Eng Rev **20,** 18 (October 1961)

[77] Stuart, H A, *Die Physik der Hochpolymeren* (Springer, Berlin, 1956), Part IV

[78] Ferry, J D, *Viscoelastic Properties of Polymers* (John Wiley and Sons, Inc, New York, 1961)

[79] Lee, E H, *Proceedings of the 1st Symposium on Naval Structural Mechanics* (Pergamon Press, New York, 1960), p 456

[80] Wiegand, J H, 'Study of mechanical properties of solid rocket propellants,'' Aerojet General Corp Rept 0411 10F (March 1962)

[81] Williams, M L, "Viscoelastic material considerations in engineering curricula,'' J Eng Educ 670 (June 1963)

[82] Prony, R, "Essai Experimentale et Analytique,'' J Ecole Polytechnique Paris **1,** 24–76 (1795)

[83] Lindsey, G H and Williams, M L, "The structural integrity of an ablating rocket subjected to axial acceleration,'' AIAA Preprint 64 151 (January 1964)